

Proteomics and Mass Spectrometry Imaging on gynaecological cancer tissue

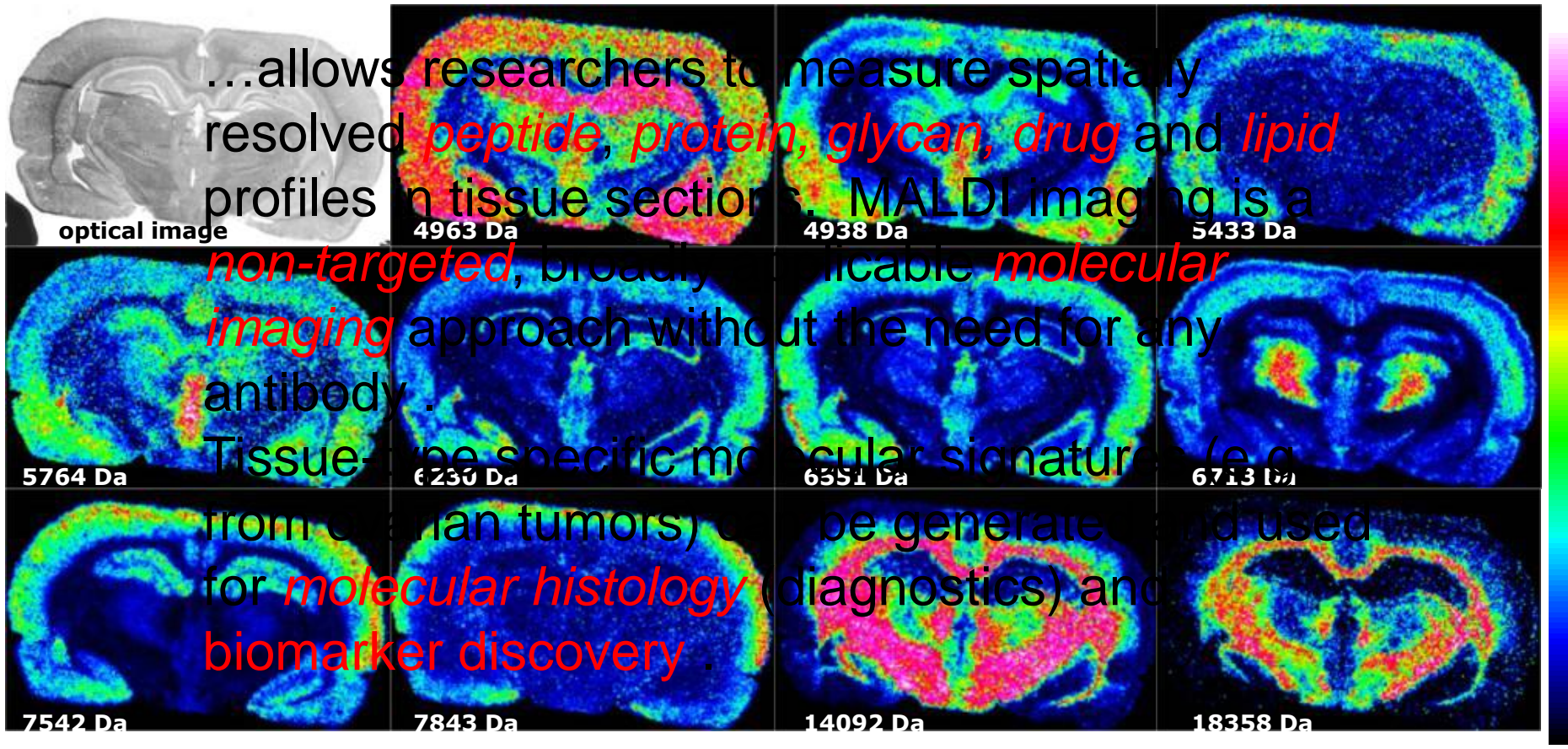
Prof Peter Hoffmann

ANZGOG 20th of March 2019

Introduction

- Mass Spectrometry Imaging analysis of Endometrial cancer FFPE tissue to distinguish from the primary tumour if the patient will have lymph node metastasis
- N-Glycan MALDI Imaging Mass Spectrometry on FFPE Ovarian Cancer Tissue changes between stage 1 and stage 3

MALDI Imaging ...



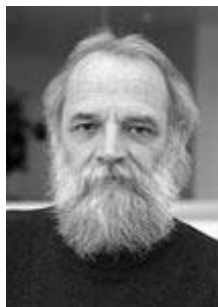
MALDI-ToF Mass spectrometry



Koichi Tanaka



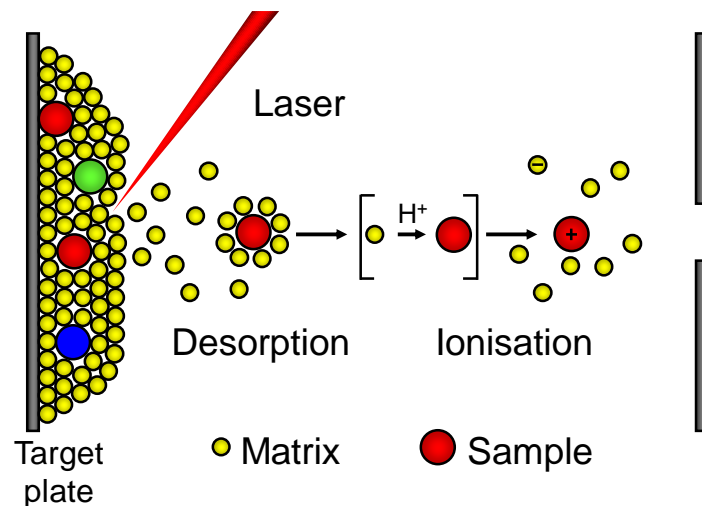
Franz Hillenkamp



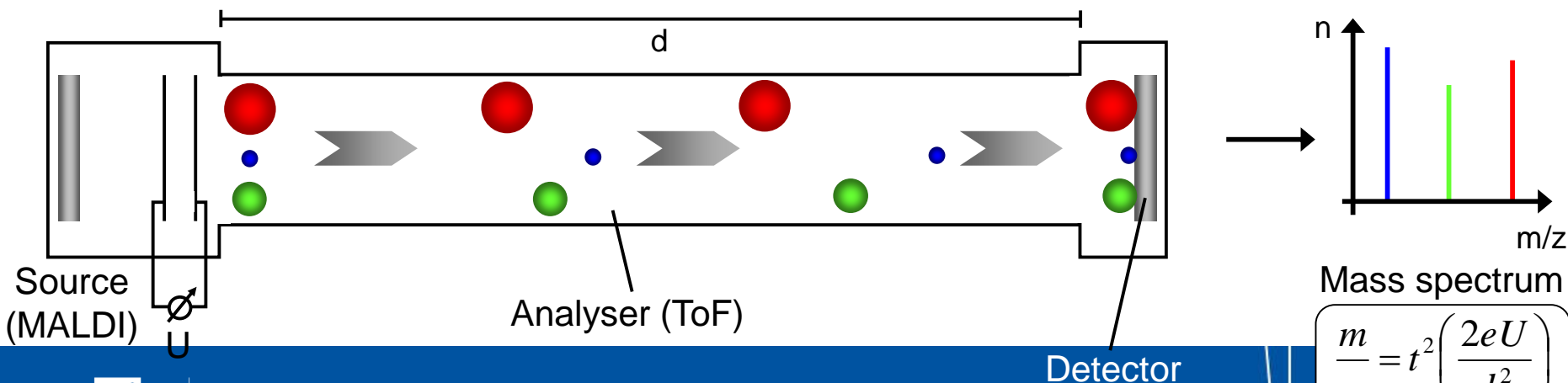
Michael Karas

Nobel price in chemistry, 2002

"for the development of methods for identification and structure analyses of *biological macromolecules*"



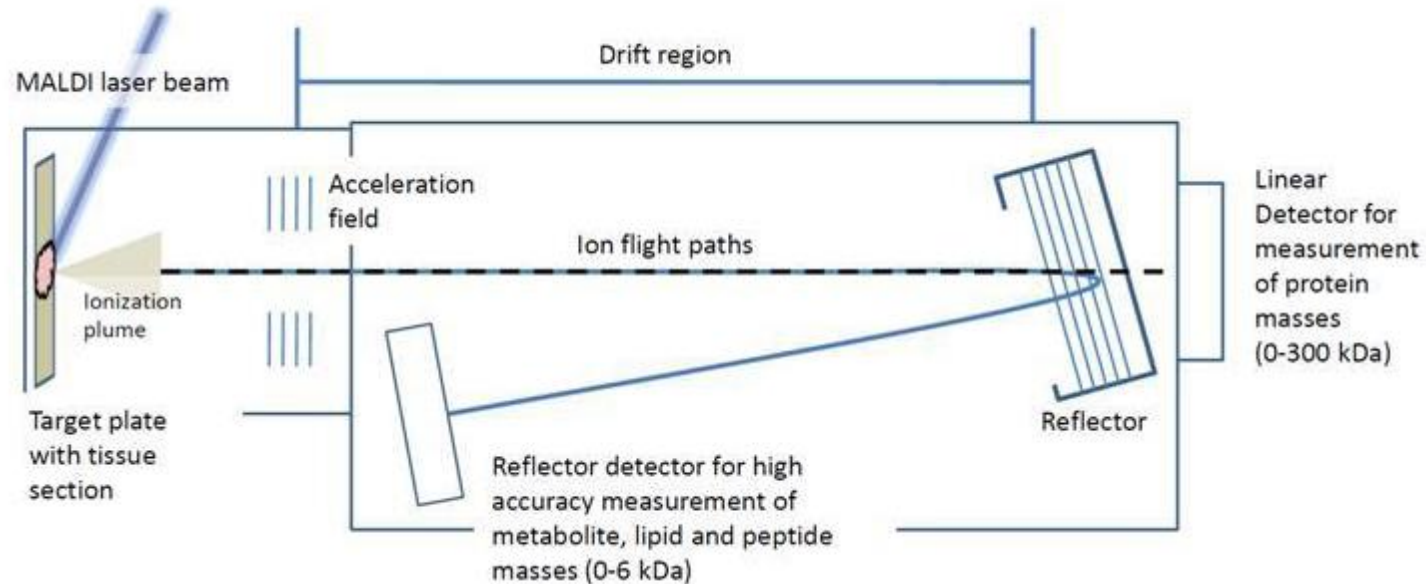
MALDI-Ionisation



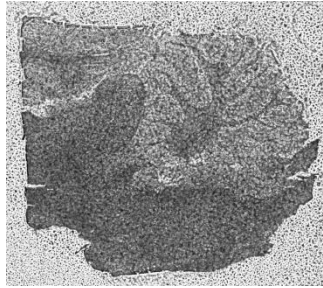
$$\frac{m}{z} = t^2 \left(\frac{2eU}{d^2} \right)$$

Time of Flight mass spectrometry

MALDI TOF/TOF MS



MALDI Imaging workflow



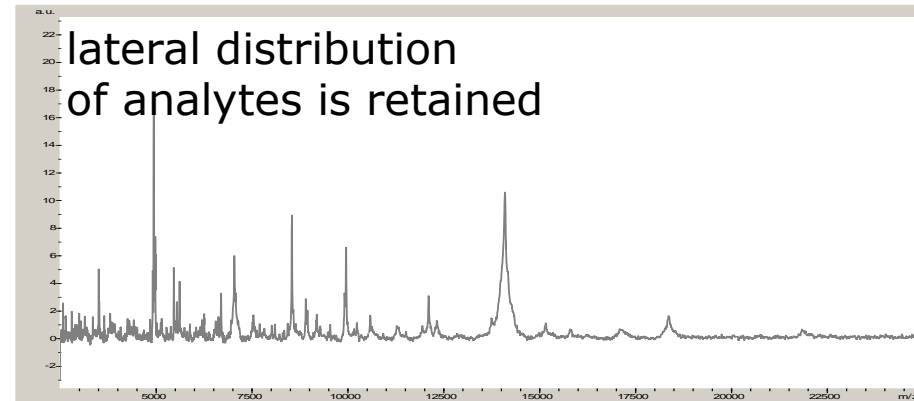
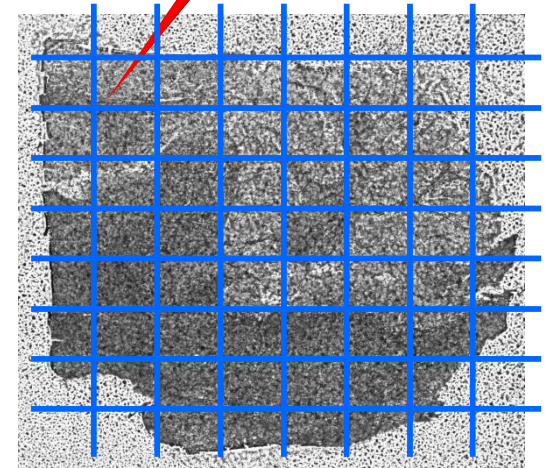
Matrix coated tissue section



MALDI target adapter for slides



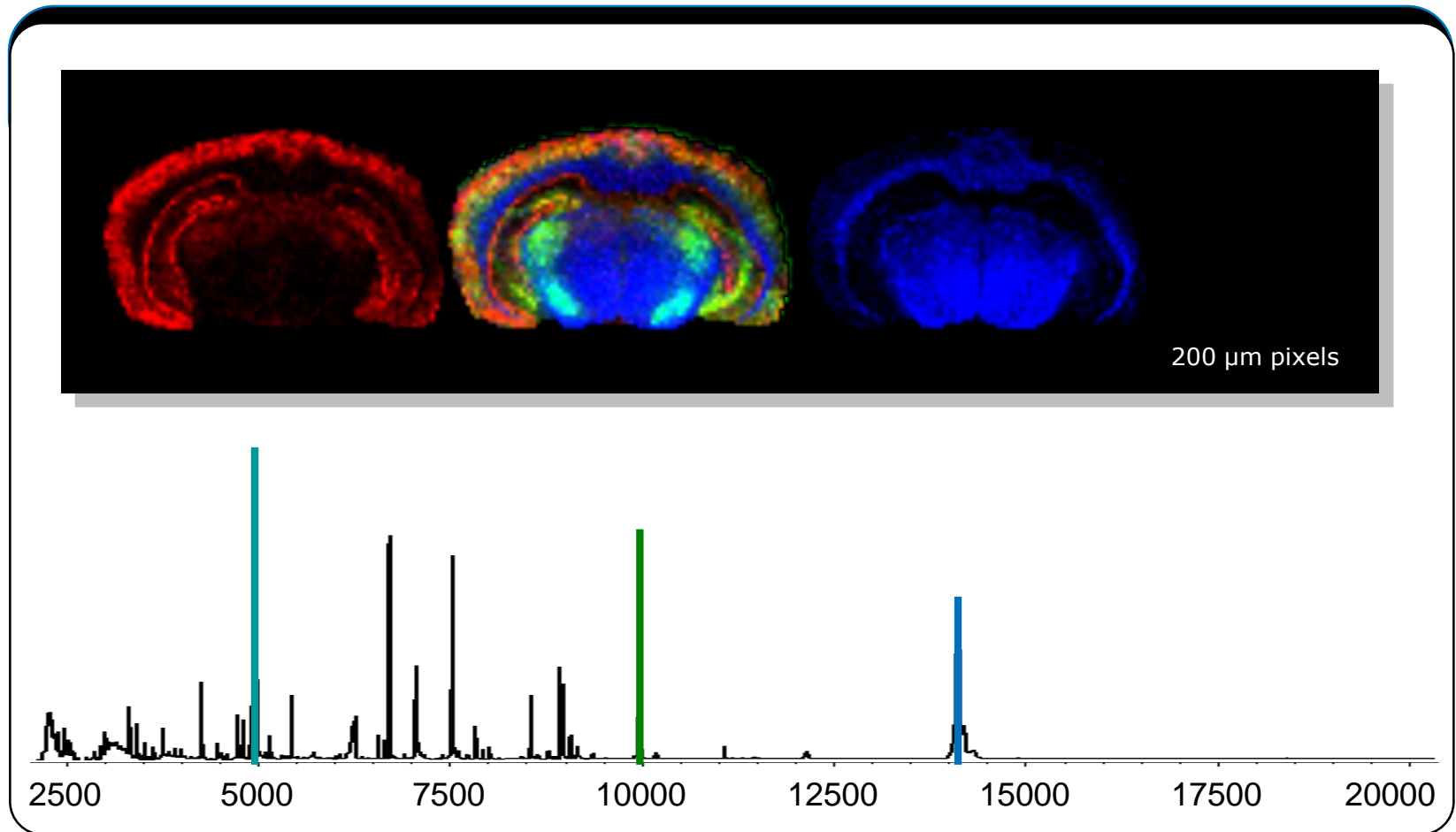
MALDI TOF/TOF MS



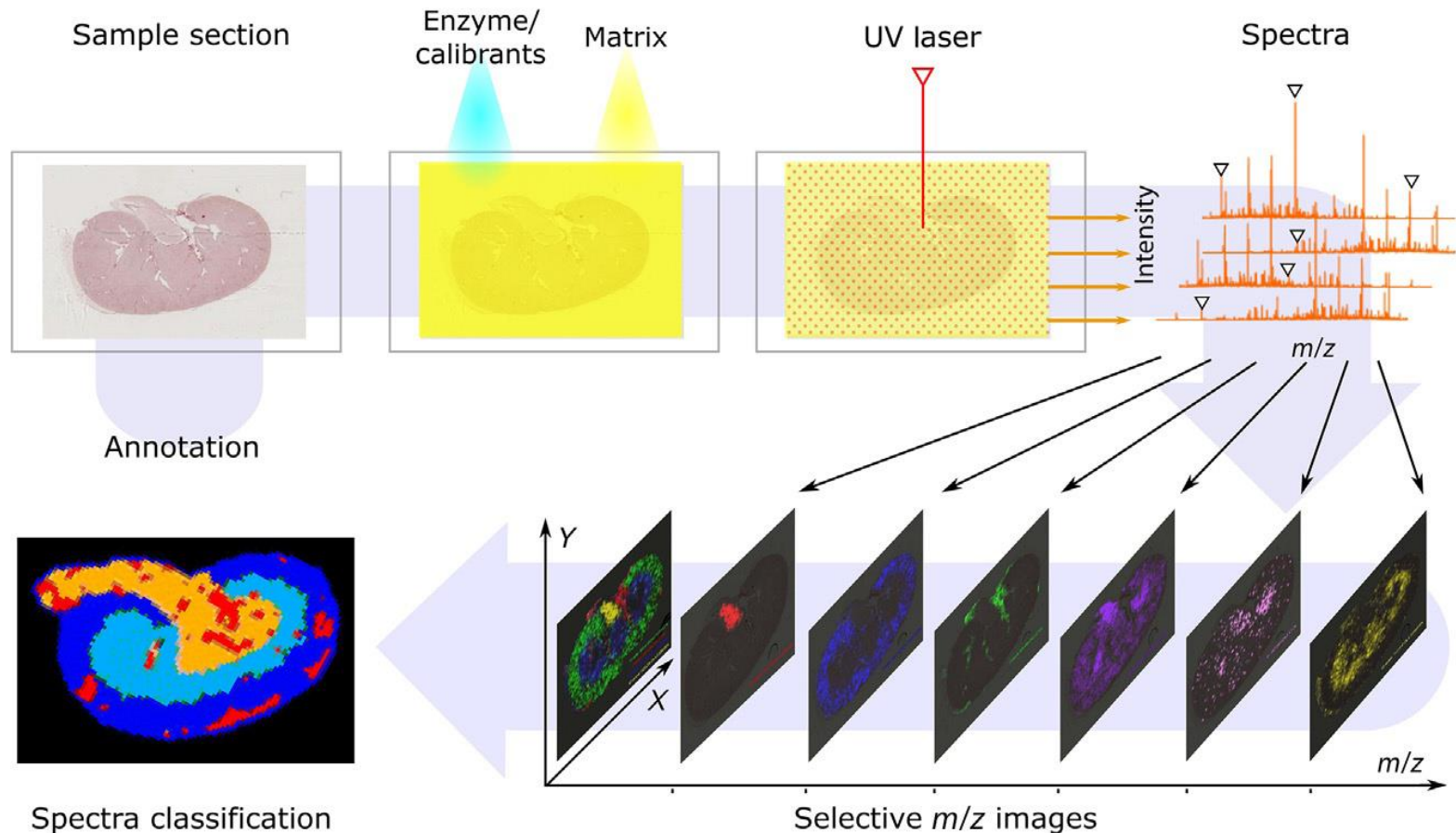
200-400
laser shots

Raster size ~80-300 μm
(=lateral resolution)

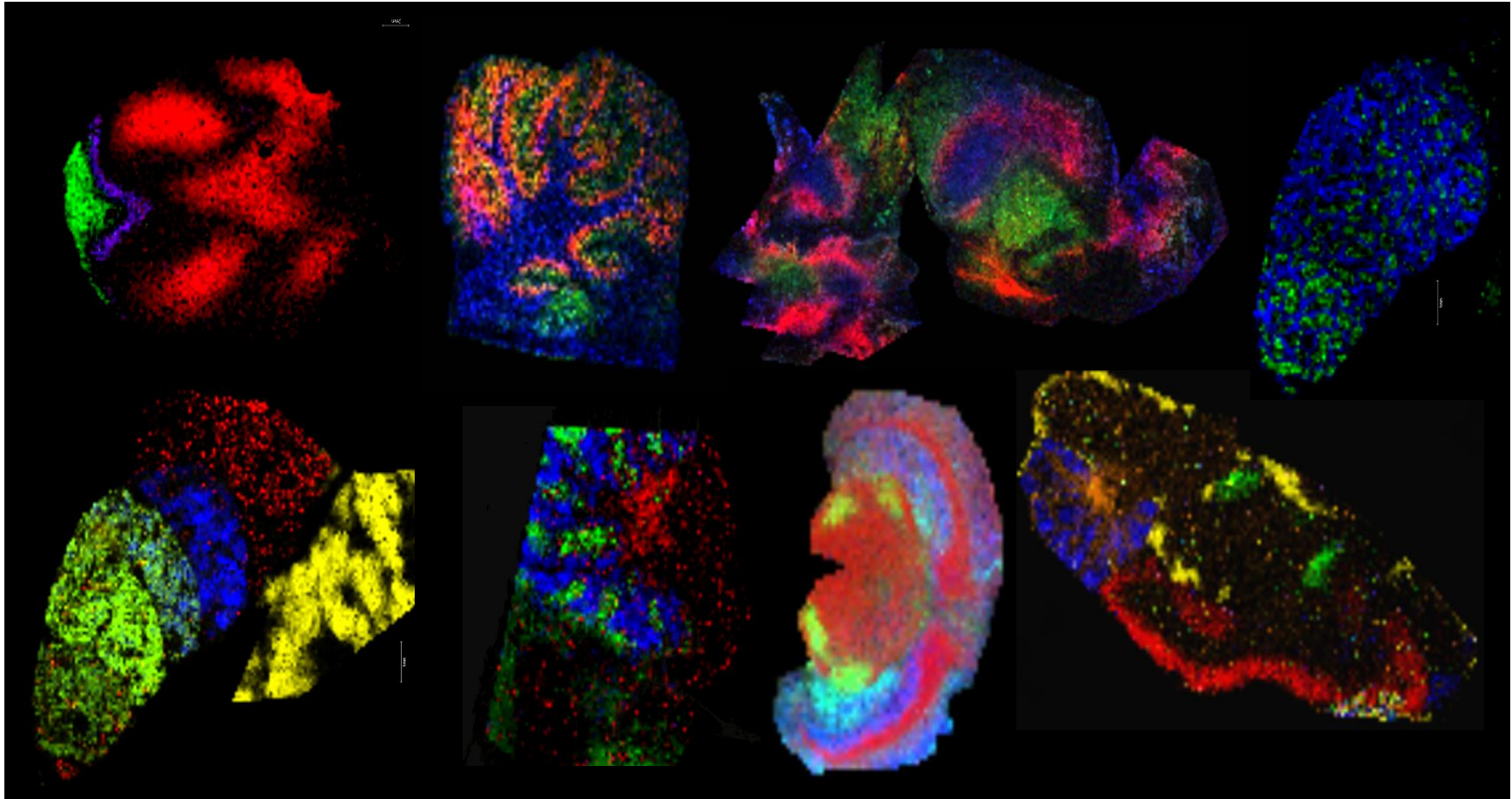
MALDI Imaging – easy multiplexing



Mass Spectrometry Imaging (MSI)



Molecular Histology by MALDI Imaging MS



Visual Microscopy by MALDI Imaging MS



“Mass spectrometry Imaging analysis of Endometrial cancer”

Parul Mittal

Peter Hoffmann, Manuela Klingler-Hoffmann, Martin K. Oehler

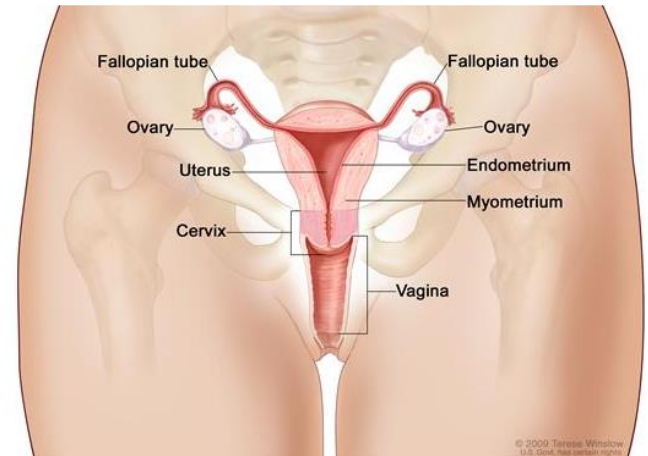
Clinical relevance

- Endometrial cancer (EC) is the most frequent malignant tumour occurring in the female reproductive system
- Affects approximately every 1/75 Australian women by the age of 75
- 5 year survival rate

Stage I	~ 85%
Stage II	~ 75%
Stage III	~ 45%
Stage IV	~ 25%

No
Metastasis

Metastasis

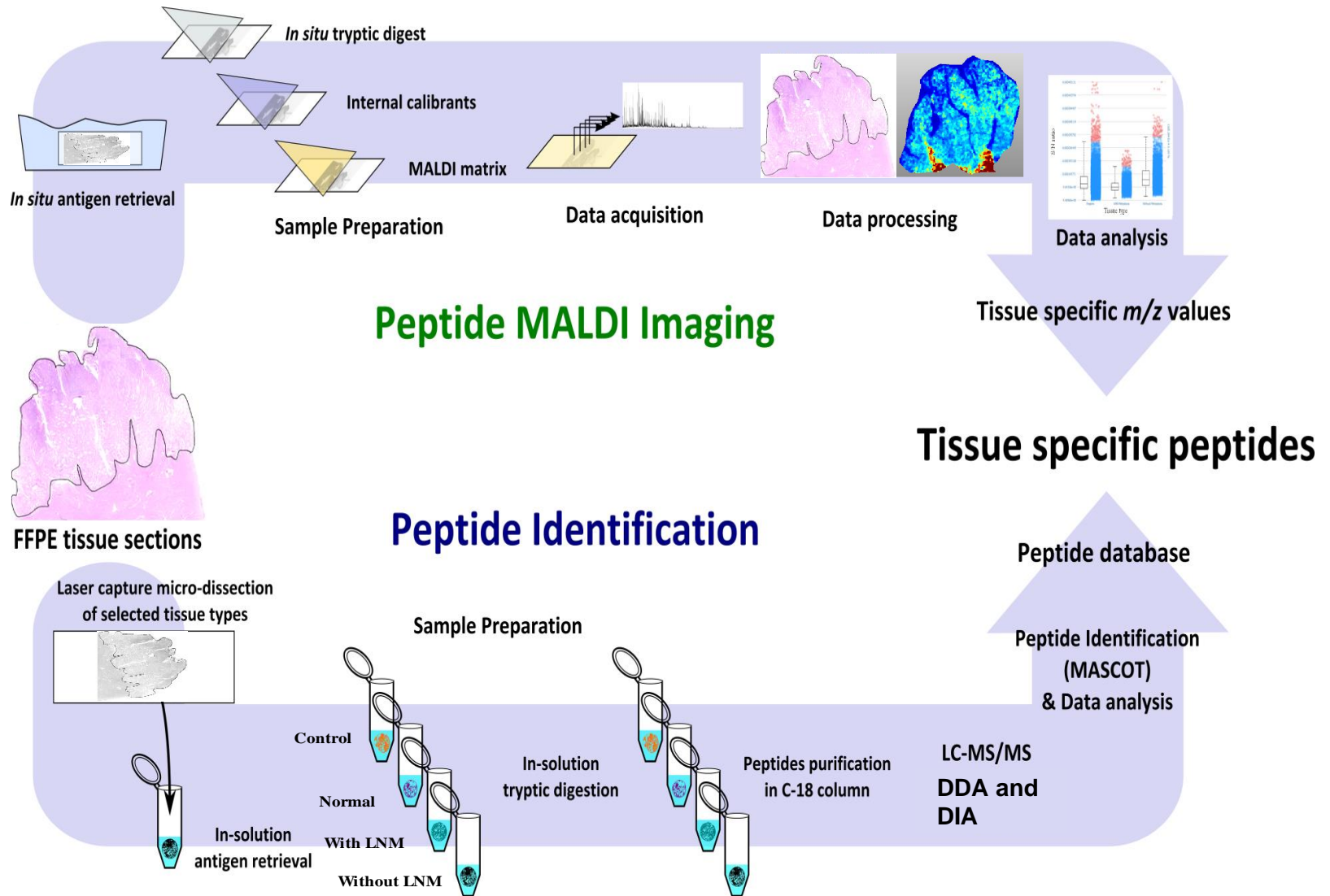


- **Most patients** with endometrial cancer routinely undergo a lymph node dissection as part of the cancer operation and postoperative lower extremity (only 10% will have lymph node metastasis)
- **Could Lymphadenectomy be safely omitted for low risk EC patients?**

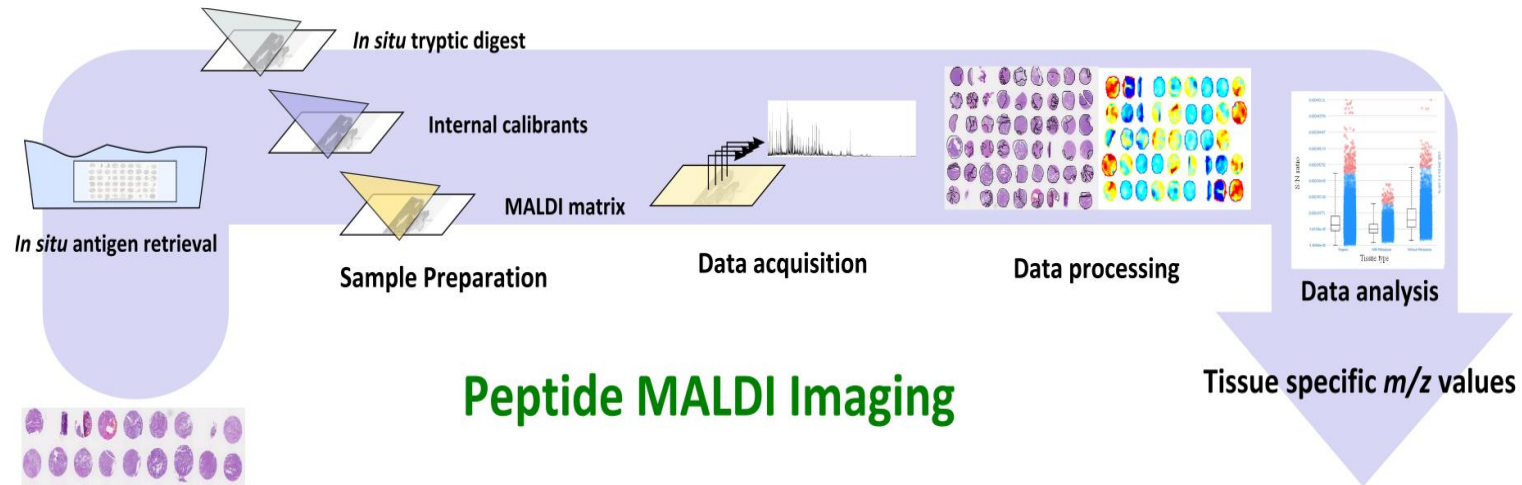
The hunt for a molecular signature

- What if we would find a molecular signature in the primary tumour which can be used to predict the metastatic potential of the tumour?
- This would change the treatment regime for patients with endometrial cancer
- Overtreatment would be prevented

MALD Imaging of FFPE tissue sections



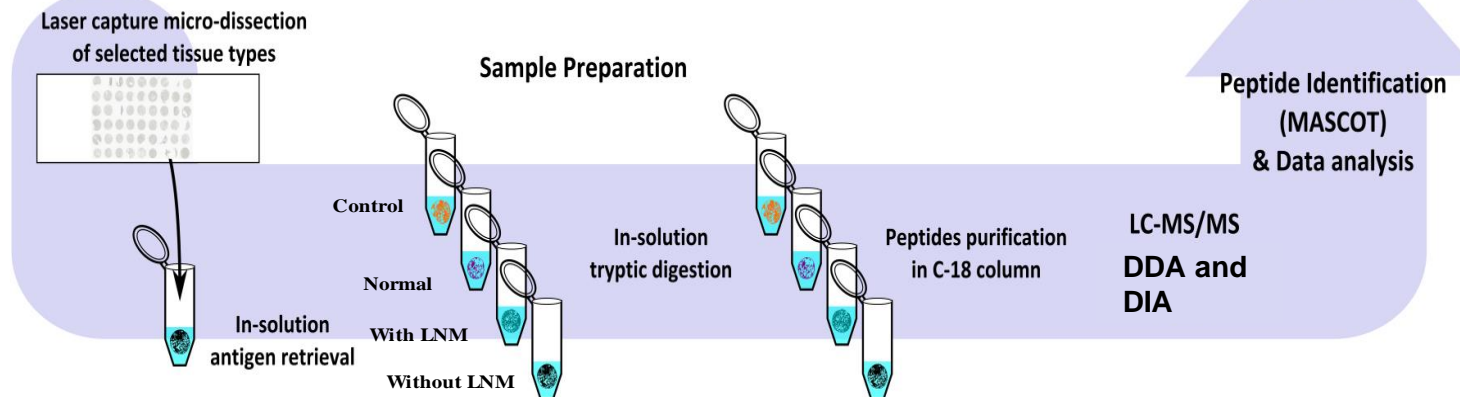
MALDI Imaging of FFPE TMA's



FFPE tissue sections

Tissue specific peptides

Peptide Identification

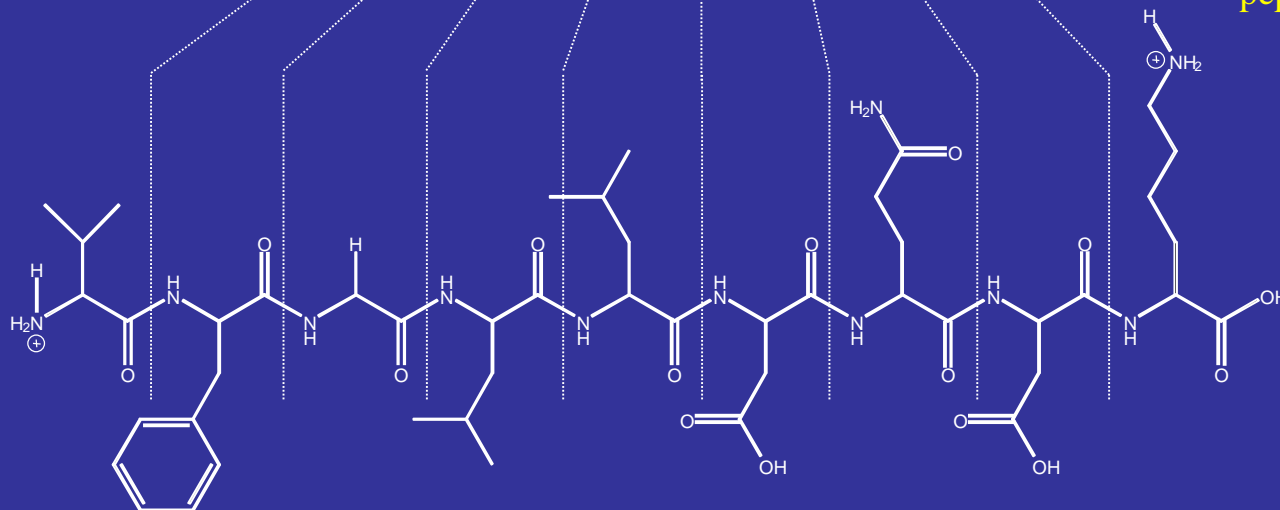


LC-MS/MS Identification

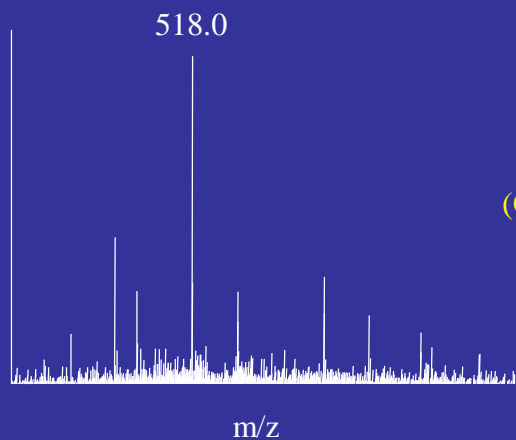
Val Phe Gly Lxx Lxx Asp Glu Asp Lys

Neutral mass of peptide is 1034 Da.

The protonated mass of the peptide, i.e., $[M+2H]^{++}$ is 1036 Da.

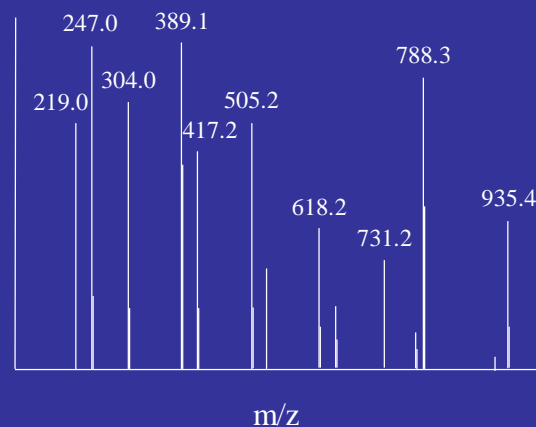


MS
Spectrum

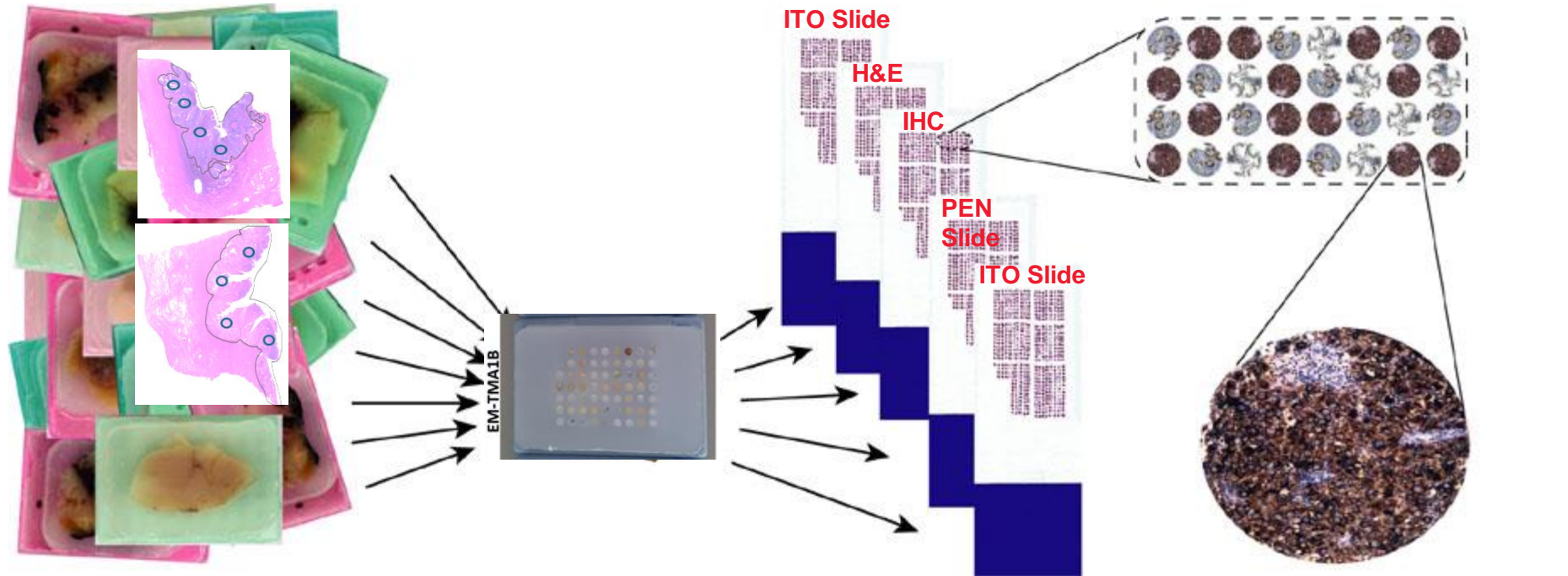


MS/MS
Spectrum

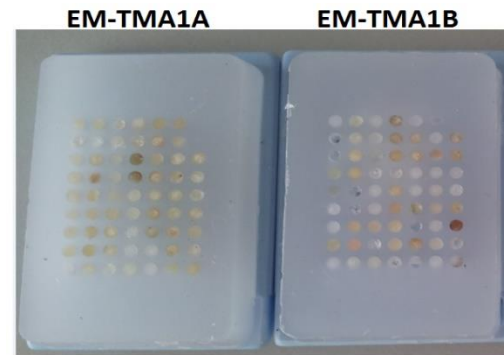
(CID of peptide ion
 m/z 518.0)



TMA construction



**EC patient samples
(n=57)**



**n = 16 with
LNM**

**n = 27 without
LNM**

n = 14

H&E stained annotated TMA1



Black: Annotated tumour region

Red: With Metastasis

Green: Without Metastasis

Blue: Excluded

Data Acquisition and Analysis

- MALDI MSI data was acquired on an ultrafleXtreme MALDI-TOF/TOF instrument
- Peak groups (intact mass, intensity) were generated from the MALDI-MSI data and then ranked using a CCA (Canonical Correlation Analysis) based method for their ability to distinguish between the primary carcinomas with and without LNM (**Lyron Winderbaum**)
- A classification accuracy of 38 out of 43 patients (88.4%) was achieved

TECHNICAL BRIEF

Classification of MALDI-MS imaging data of tissue microarrays using canonical correlation analysis-based variable selection

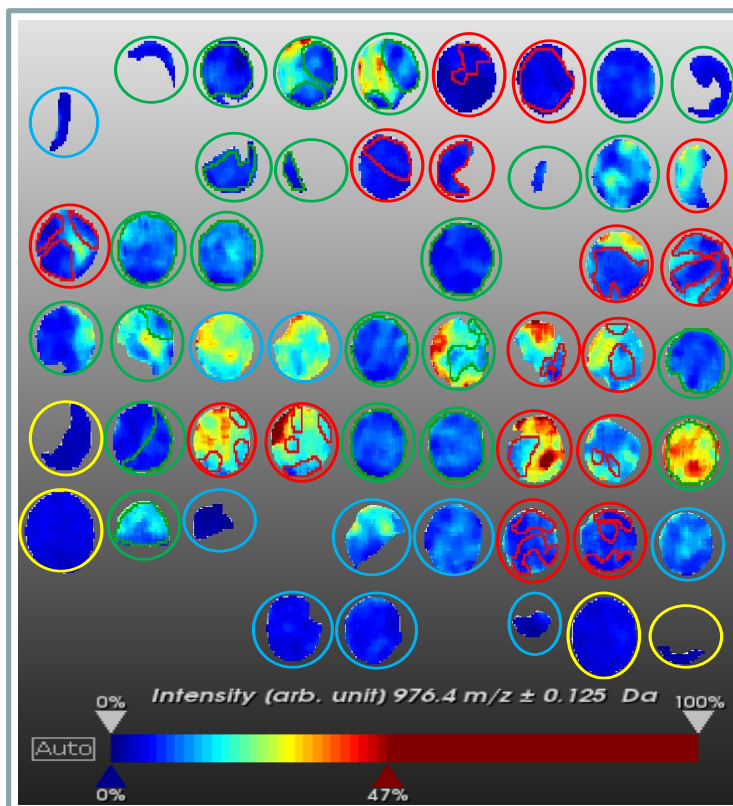
Lyron Winderbaum, Inge Koch, Parul Mittal and Peter Hoffmann

The University of Adelaide, Adelaide, SA, Australia

Top ranked m/z peak groups as ranked by the CCA

Ranked m/z values by CCA	Protein Accession Name
967.417	PLEC_HUMAN
1157.667	CPNE1_human
1198.667	ACTA_HUMAN
802.417	no match
975.417	RL11_human
1242.667	HS90B_human
1161.667	ACTA_HUMAN
1167.667	HNRPM_human
1612.917	CLH1_human
1032.667	RS9_human
1027.667	PGM1_human
941.417	CPNE3_human
976.417	ACTA_HUMAN
1406.667	SAMP_human
1138.667	EF2_human
1115.417	EIF3E_human
944.417	H2A1D_human
857.417	No match
1905.917	HSPB1_human
915.417	COCOA1_human

Mittal et al. 2016, Proteomics

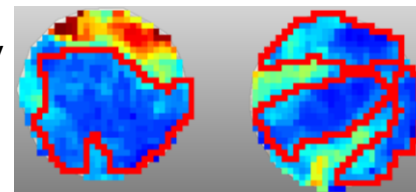


H&E stain

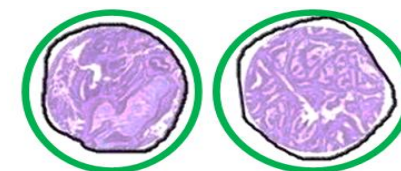


With
LNM

Ion intensity
images

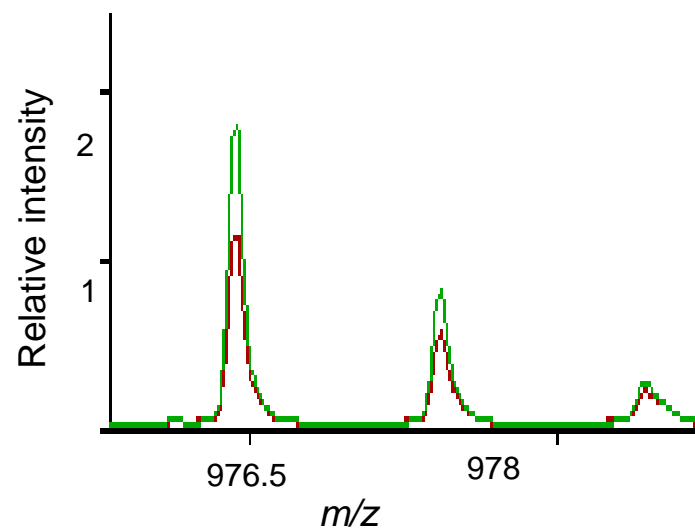
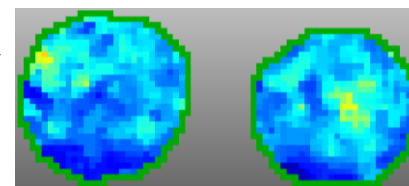


H&E stain



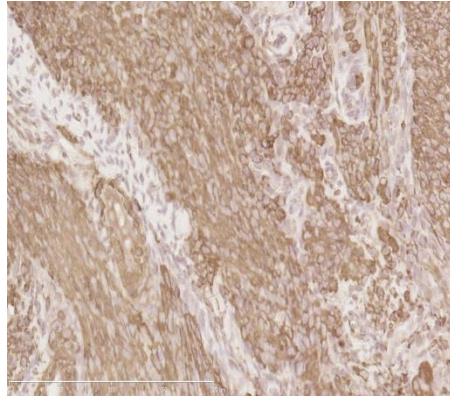
Without
LNM

Ion intensity
images

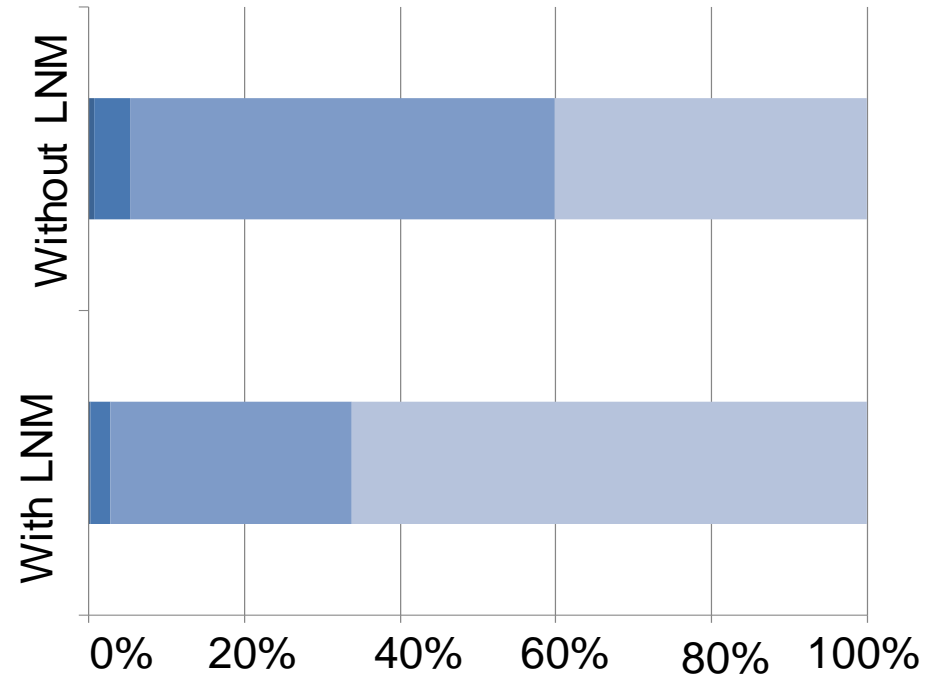
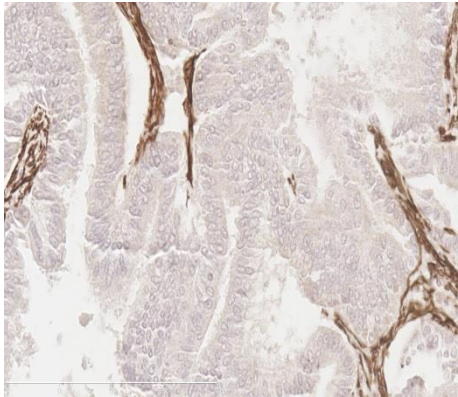


Validation by Immunohistochemistry

Without
LNM



With
LNM



■ High positive ■ Positive
■ Low positive ■ Negative

Mittal et al. 2016, Proteomics

RESEARCH ARTICLE

Lymph node metastasis of primary endometrial cancers: Associated proteins revealed by MALDI imaging

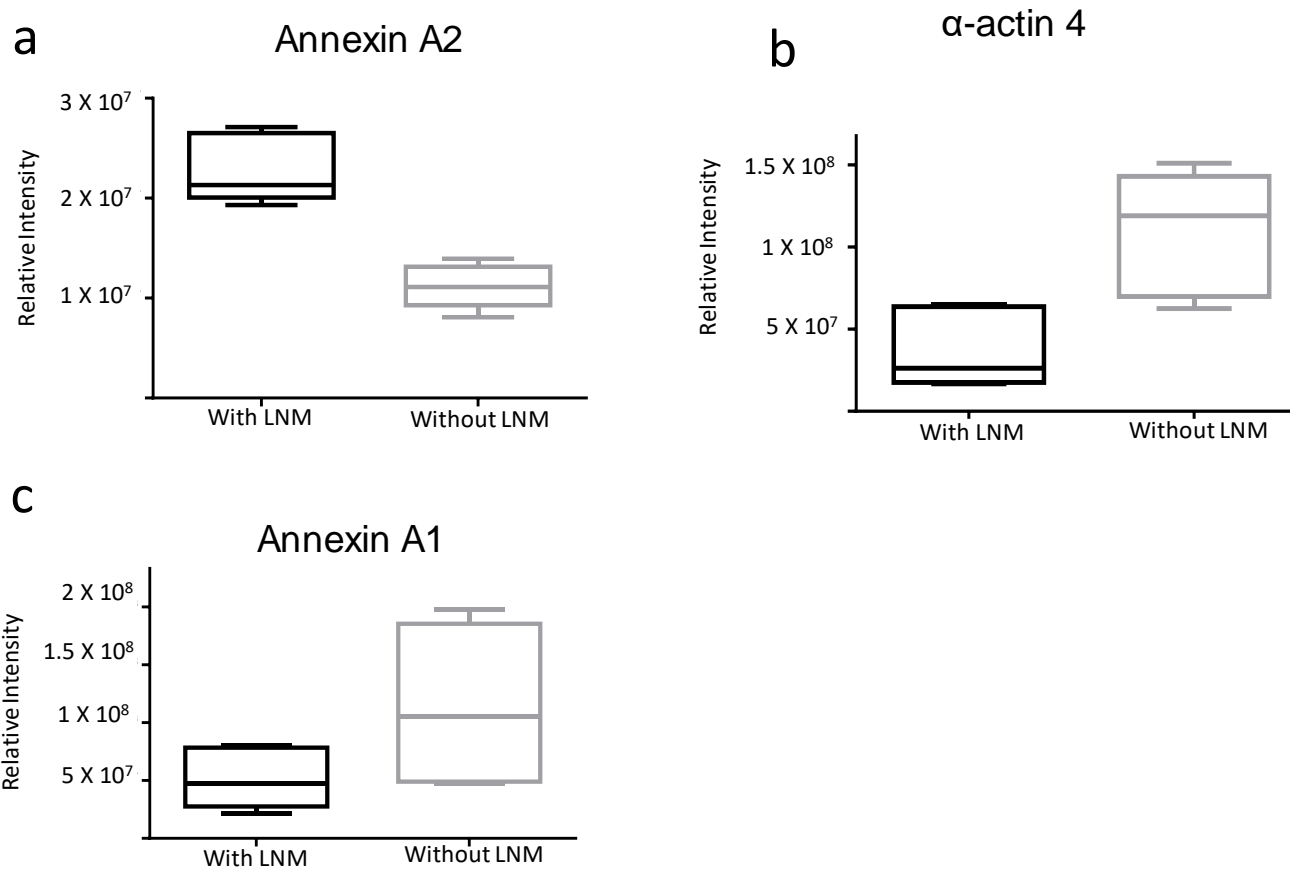
Parul Mittal^{1,2*}, Manuela Klingler-Hoffmann^{1,2*}, Georgia Arentz^{1,2}, Lyron Winderbaum^{1,2},
Noor A Lokman^{1,8}, Chao Zhang^{1,2}, Lyndal Anderson³, James Scurry⁴, Yee Leung⁵,
Colin JR Stewart⁵, Jonathan Carter⁶, Gurjeet Kaur⁷, Martin K. Oehler^{8,9}
and Peter Hoffmann^{1,2**}

TCGA

- The Cancer Genome Atlas, established in 2005
- High throughput data for genomic and proteomic analysis
- Databank contained 514 EC patients, with RNA sequencing data available for 333 patients (n=54 with LNM and n=279 without LNM)
- From the analysis, we have chosen eleven differentially expressed genes: six most significant up- and five down-regulated genes
- Following extensive literature review the list has grown to 60 target proteins, which might be differentially expressed in primary tumours with and without LNM

- Using traditional form of LC-MS/MS, we were able to detect 23 of these proteins in EC tissue cohort (**n=5 with LNM** and **n=5 without LNM**)
- Using targeted LC-MS/MS, we confirmed the differential expression of 5 of the proteins (more than 2 peptides and p value < 0.05)
 - Annexin A2
 - Annexin A1
 - Alpha actinin 4
 - EGFR
 - ERBB2

Relative quantification by targeted LC-MS/MS

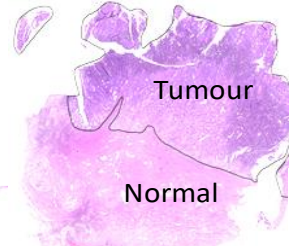
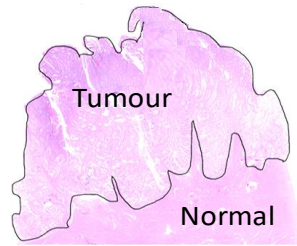


Spatial localization by MALDI MSI

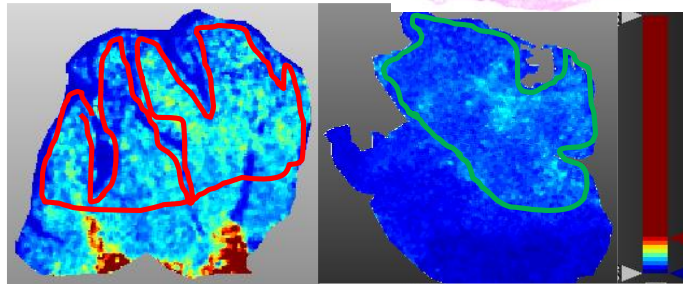
- The tissue localization of peptides from the differentially expressed proteins were visualized using MALDI MSI in whole tissue sections (**n=5 with LNM** and **n=5 without LNM**) as well as TMAs (**n=16 with LNM** and **n=27 without LNM**)

With LNM

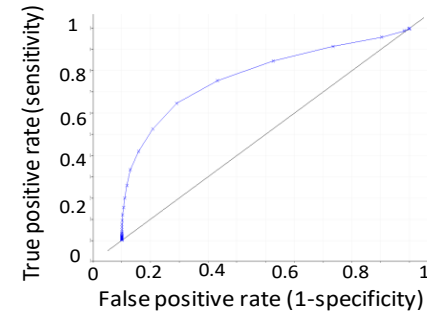
Without LNM



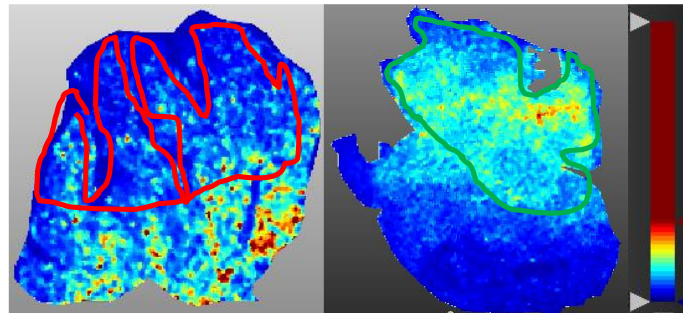
Annexin
A2



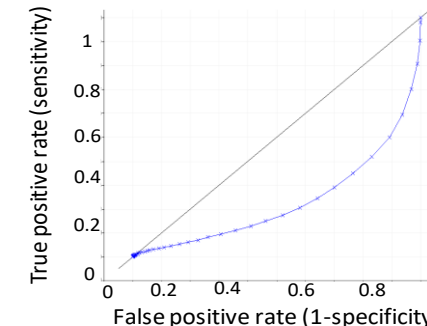
AUC = 0.780, 1542.831 $m/z \pm 0.125$ Da



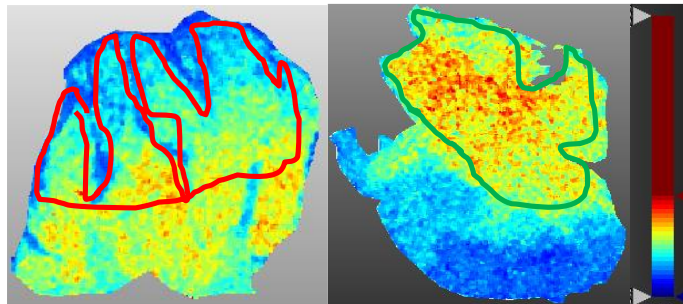
α -actin 4



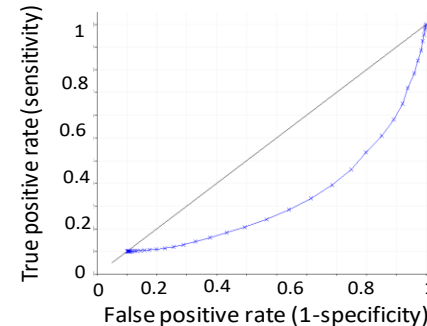
AUC = 0.229, 1429.76 $m/z \pm 0.125$ Da



Annexin
A1

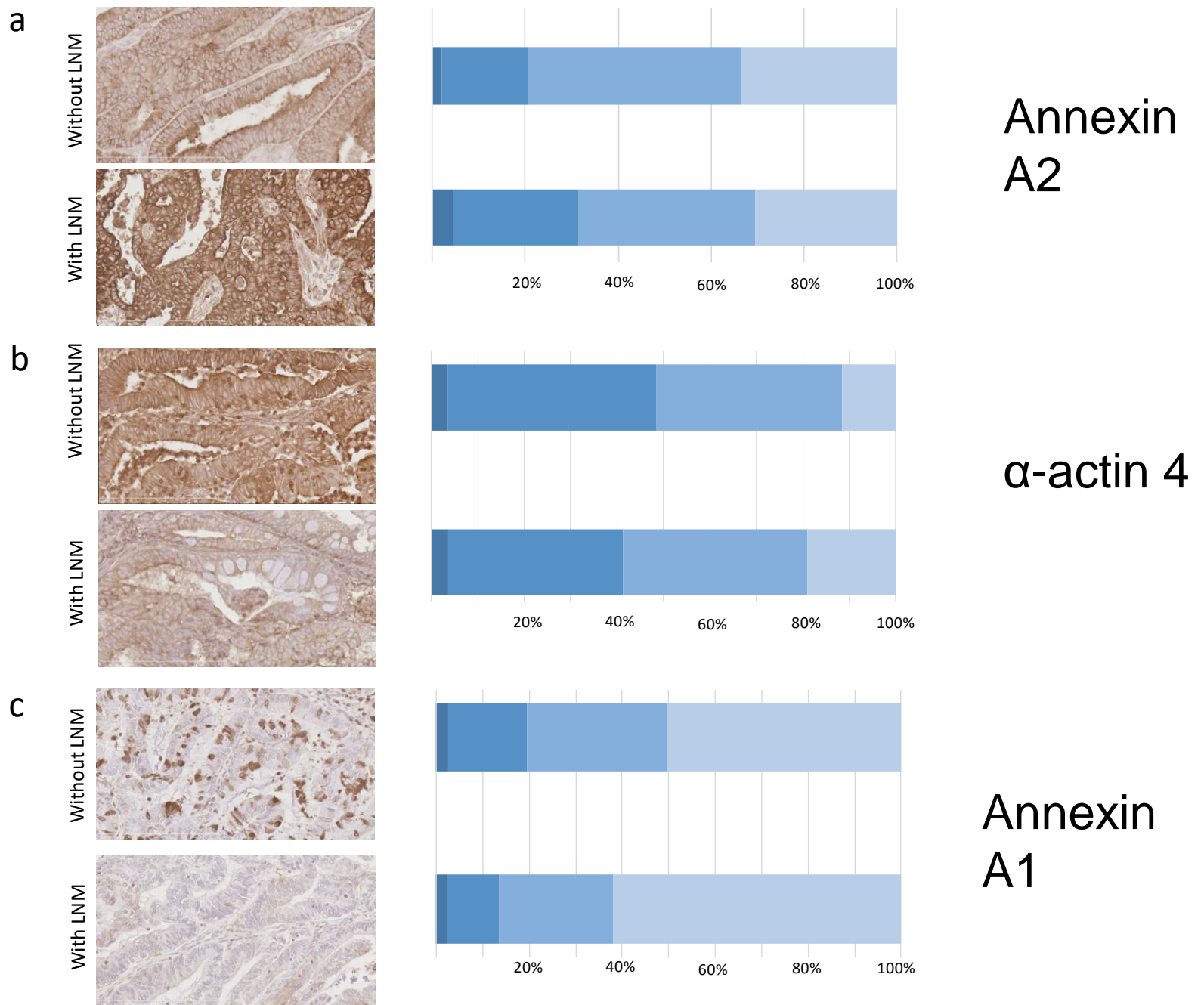


AUC = 0.240, 1099.591 $m/z \pm 0.125$ Da

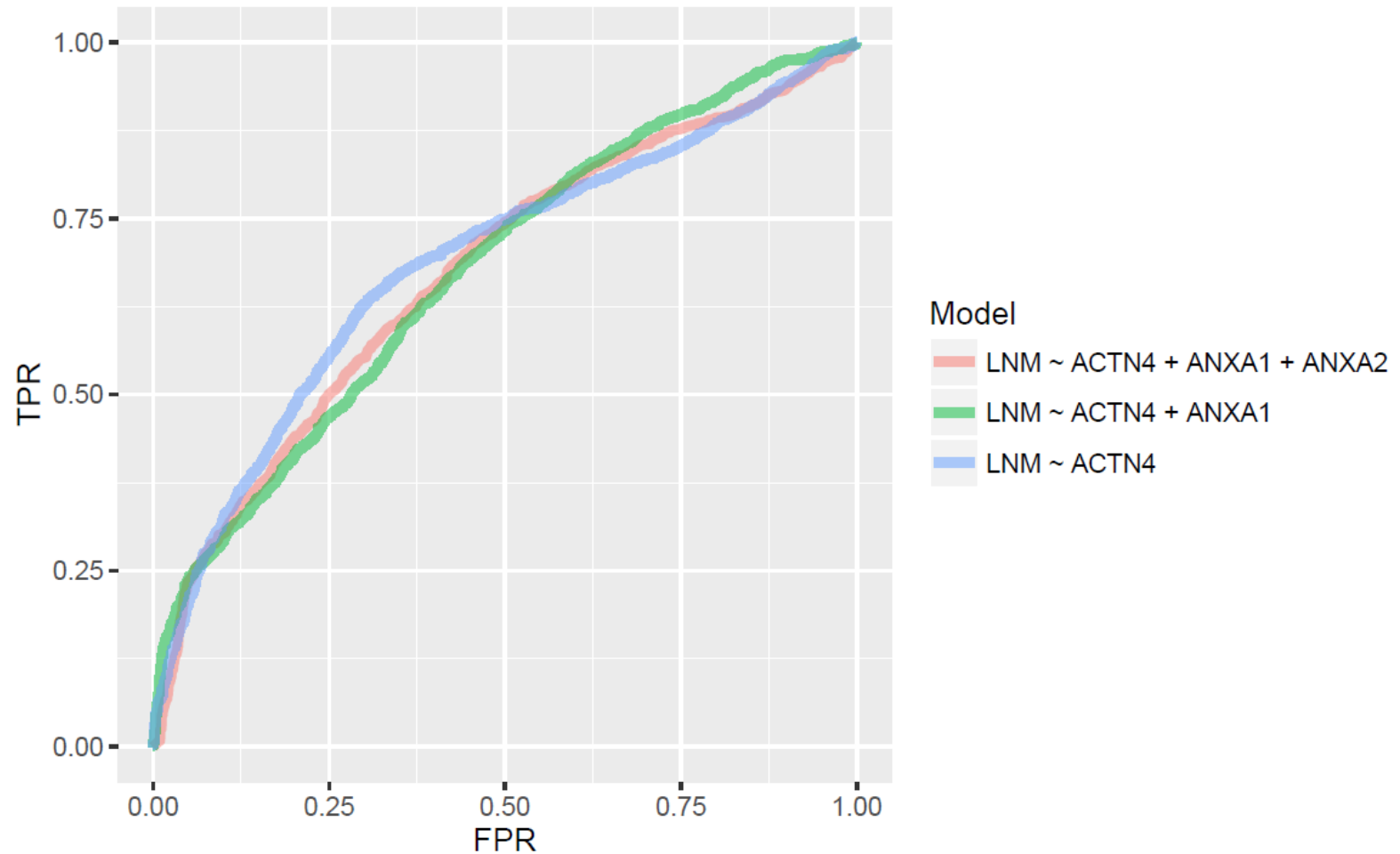


Validation by Immunohistochemistry

- The proteins identified were further validated by immunohistochemistry
- This allowed the simultaneous analysis of 43 patients (n=16 with LNM and n=27 without LNM) of which 39 had not been analysed by relative quantification LC-MS/MS.



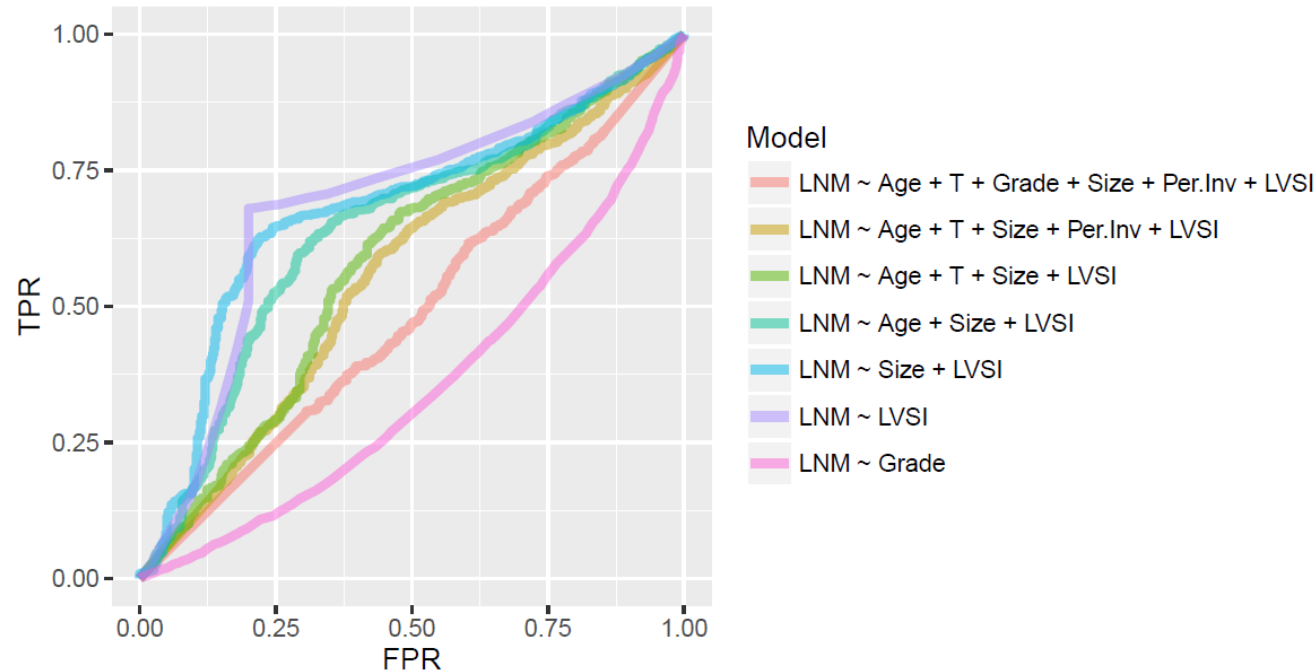
Logistic Regression Model to fit IHC results



Nomogram using clinical variables

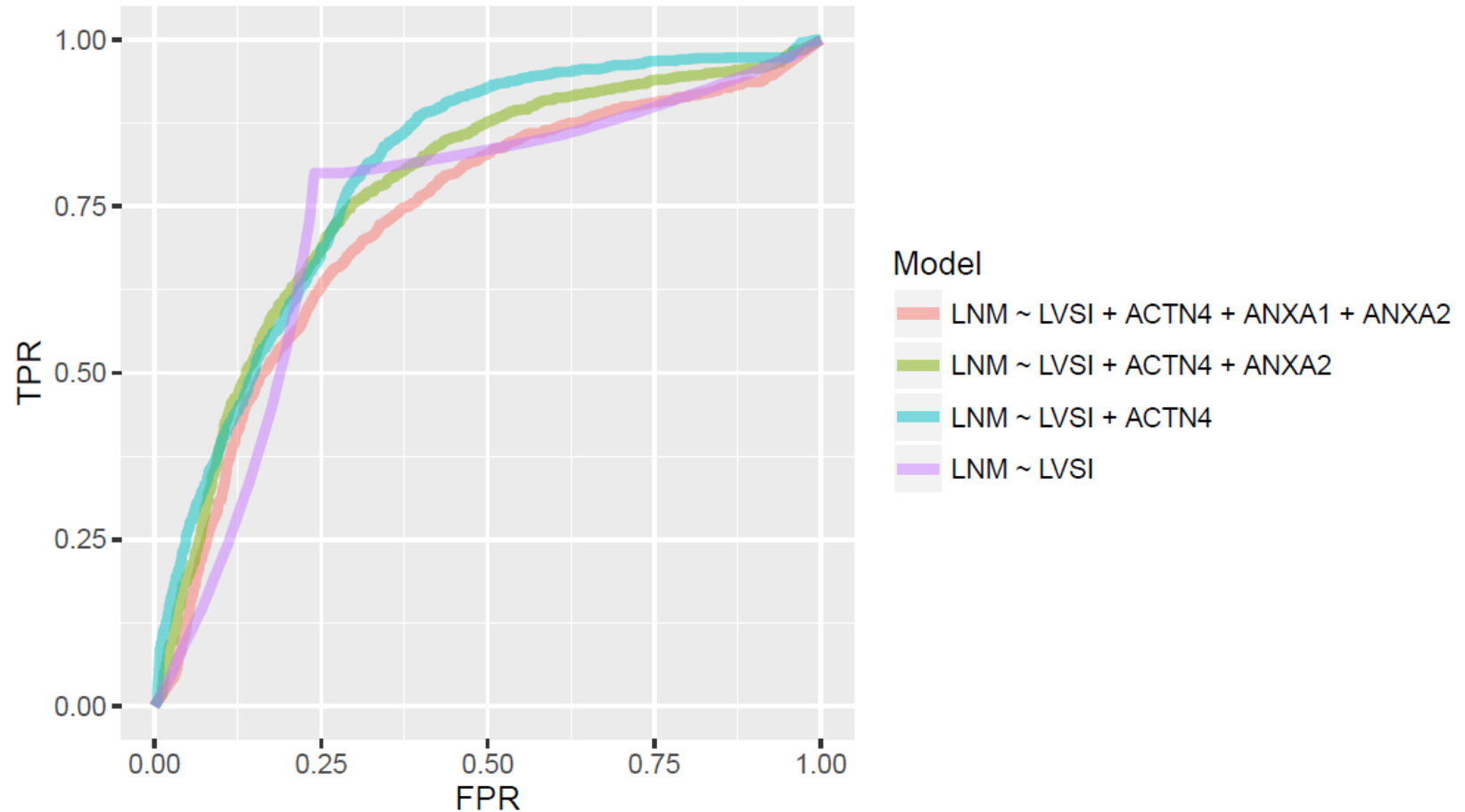
- From the 43 patients analysed, we had 35 patients for which all the following clinical variables have been recorded: age, tumour grade, tumour size, tumour extent, and lympho-vascular space invasion (LVSI)
- Fitting a logistic regression model based on all these clinical variables and iteratively removing the least significant of them
- Resulted in only one significant clinical variable: LVSI, and this agrees with recently published results

Model to fit clinical variables

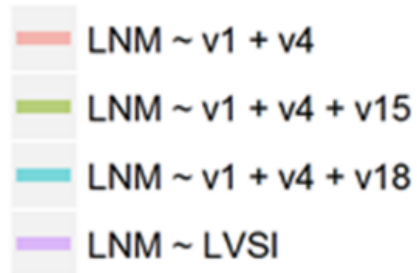
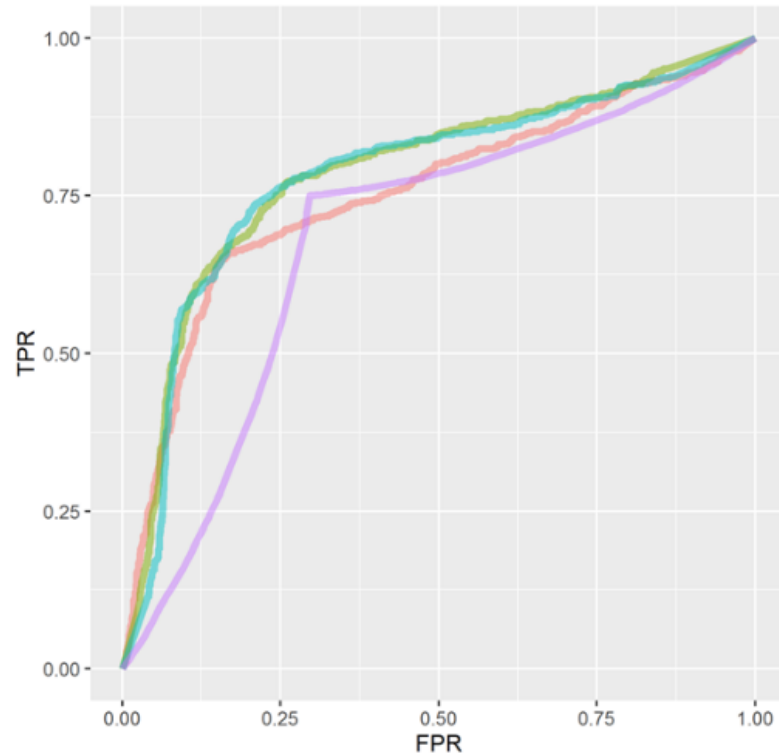


	Model	AUC
	LNM ~ Age + T + Grade + Size + Per.Inv + LVSI	0.49
	LNM ~ Age + T + Size + Per.Inv + LVSI	0.56
	LNM ~ Age + T + Size + LVSI	0.58
	LNM ~ Age + Size + LVSI	0.64
	LNM ~ Size + LVSI	0.68
	LNM ~ LVSI	0.68
	LNM ~ Grade	0.35

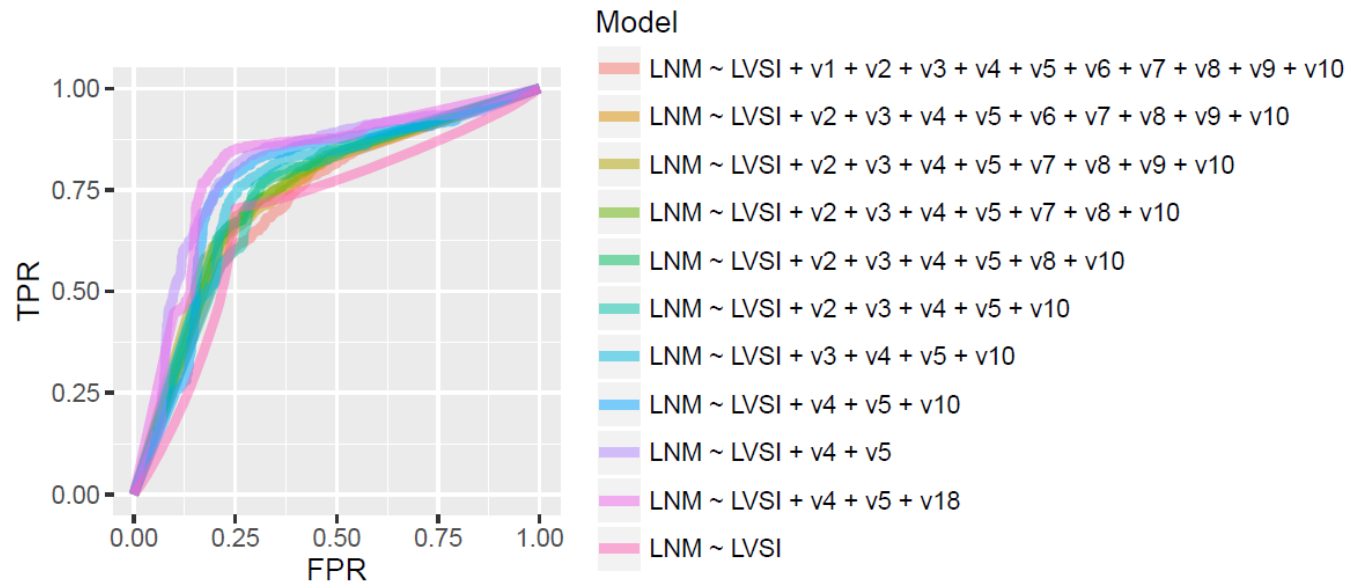
Model to fit LVSI and IHC results



Model to fit MALDI-MSI variables alone



Adding MALDI-MSI Variables with LVSI



	Model	AUC
LNM ~ LVSI + v1 + v2 + v3 + v4 + v5 + v6 + v7 + v8 + v9 + v10		0.72
LNM ~ LVSI + v2 + v3 + v4 + v5 + v6 + v7 + v8 + v9 + v10		0.74
LNM ~ LVSI + v2 + v3 + v4 + v5 + v7 + v8 + v9 + v10		0.75
LNM ~ LVSI + v2 + v3 + v4 + v5 + v7 + v8 + v10		0.74
LNM ~ LVSI + v2 + v3 + v4 + v5 + v8 + v10		0.75
LNM ~ LVSI + v2 + v3 + v4 + v5 + v10		0.74
LNM ~ LVSI + v3 + v4 + v5 + v10		0.76
LNM ~ LVSI + v4 + v5 + v10		0.77
LNM ~ LVSI + v4 + v5		0.81
LNM ~ LVSI + v4 + v5 + v18		0.82
LNM ~ LVSI		0.69

Nomogram for Endometrial Cancer

M. Koskas et al. / European Journal of Cancer 61 (2016) 52–60

57

Table 3
Evaluation of postoperative and preoperative models.

Model	Number of patients	Observed LNM probability	Predicted LNM probability (%)	AUC	E _{aver} (%)	E _{max} (%)	FN rate	Patients assigned to the low-risk group
Kamura <i>et al.</i> 1999 [4]	316	41/316 (13.0%)	8.4	0.72	4.7	7.5%	NA	NA
French nomogram [3,8]	447	84/447 (18.8%)	11.3	0.78	7.7	15.3	10/206 (4.9%)	206/447 (46.1%)
Milam <i>et al.</i> 2012 [5]	283	28/283 (9.9%)	9.3	0.73	3.2	26.1	0/24 (0%)	24/283 (8.4%)
Zhang <i>et al.</i> 2012 [18]	285	46/285 (16.1%)	NA	NA	NA	NA	2/67 (3.0%)	67/285 (23.5%)
GOG criteria [6]	330	39/330 (11.8%)	12.0	0.76	2.0	8.3	0/18 (0%)	18/330 (5.4%)
Mayo clinic nomogram [7]	182	28/182 (15.4%)	21.9	0.75	5.5	23.0	1/39 (2.6%)	39/182 (21.4%)
Akbayir <i>et al.</i> [17]	229	36/229 (15.7%)	NA	NA	NA	NA	3/86 (3.5%)	86/229 (37.6%)
KGOG model [9]	160	27/160 (16.9%)	13.1	0.76	3.6	4.8	3/68 (4.4%)	68/160 (42.5%)
Lee <i>et al.</i> 2010 [10]	201	41/201 (20.4%)	20.2	0.66	5.6	64.2	5/54 (9.2%)	54/201 (26.9%)
Todo <i>et al.</i> 2007 [11,19]	184	38/184 (20.7%)	19.2	0.66	6.7	16.3	4/52 (7.7%)	52/184 (28.3%)

Abbreviations: AUC, area under the receiver operating characteristic curve; LNM, lymph node metastasis; NA, not assessable; E, difference in predicted and calibrated probabilities between calibration and AUC; E_{max}, maximal error; E_{aver}, average error; FN, false negative.

LNM: LVSI + v4 + v5 + v18 0.82

LNM: LVSI + v4 + v5 0.81

Summary

- LVSI information not available when women are diagnosed with EC as they have only small biopsy taken
- Would be great to have a model to guide the surgeons whether to remove the lymph nodes before the surgery.
- MALDI MSI in combination with LVSI performs better to predict LNM from primary tumours for endometrial cancer than anything else available

N-Glycan MALDI Imaging Mass Spectrometry on FFPE Ovarian Cancer Tissue

Matthew T. Briggs

Peter Hoffmann, Nicki Packer, Martin Oehler

Ovarian Cancer (OC)

The most fatal gynaecological malignancy in adult women

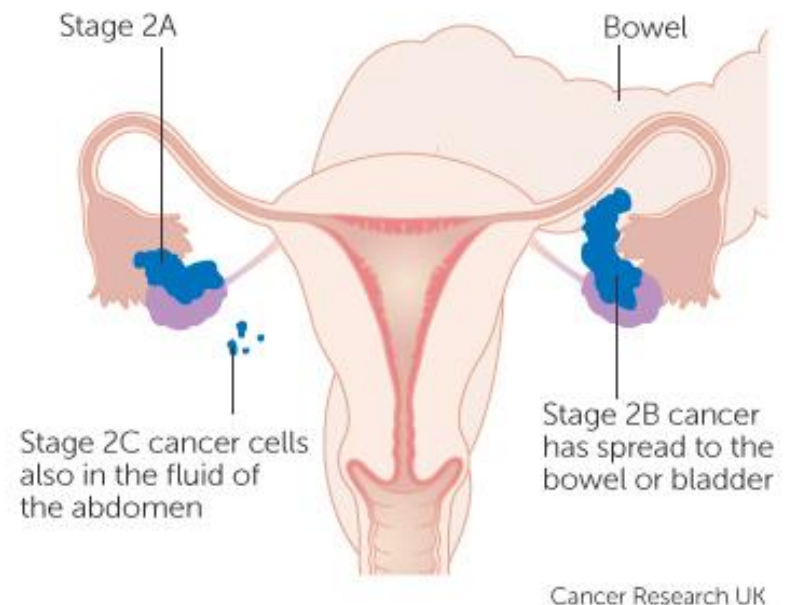
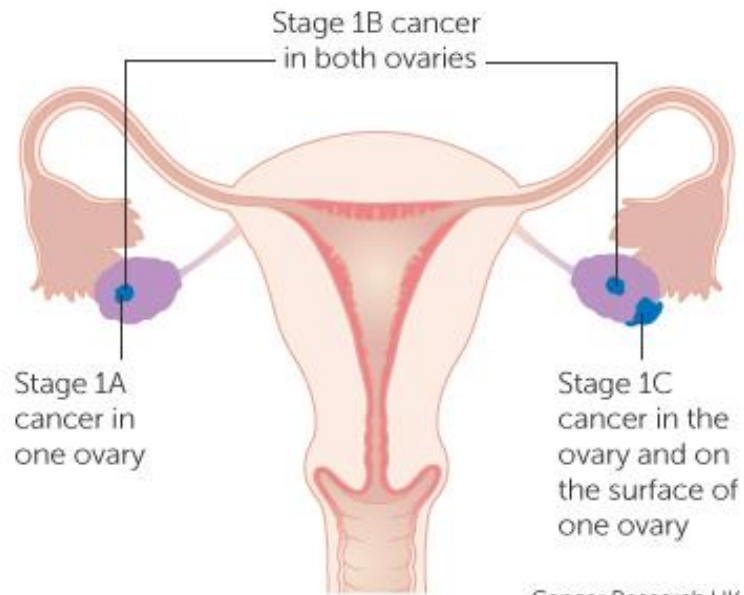
- Asymptomatic in early stages
- Diagnosed in late-stages
- Leads to metastasis

In Australia during 2018, there is estimated to be

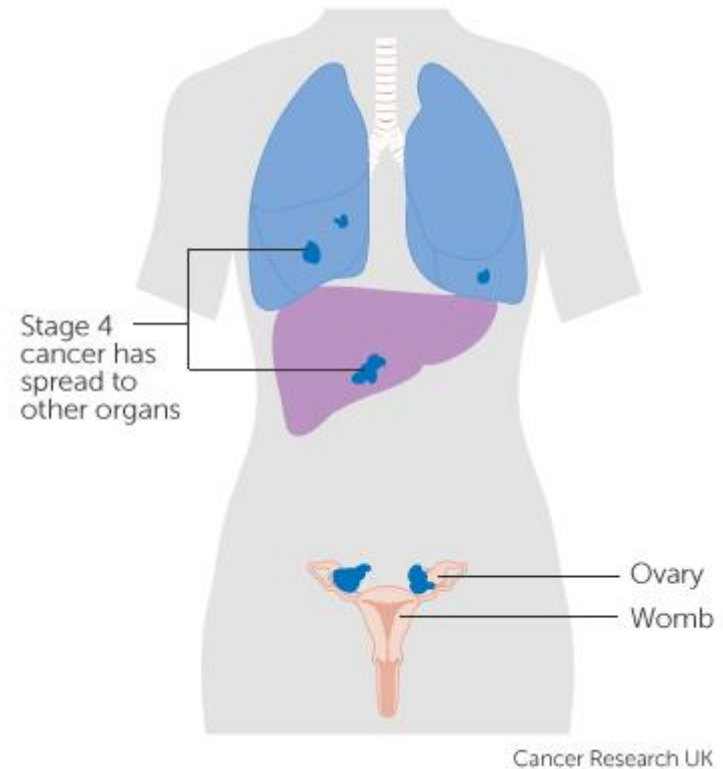
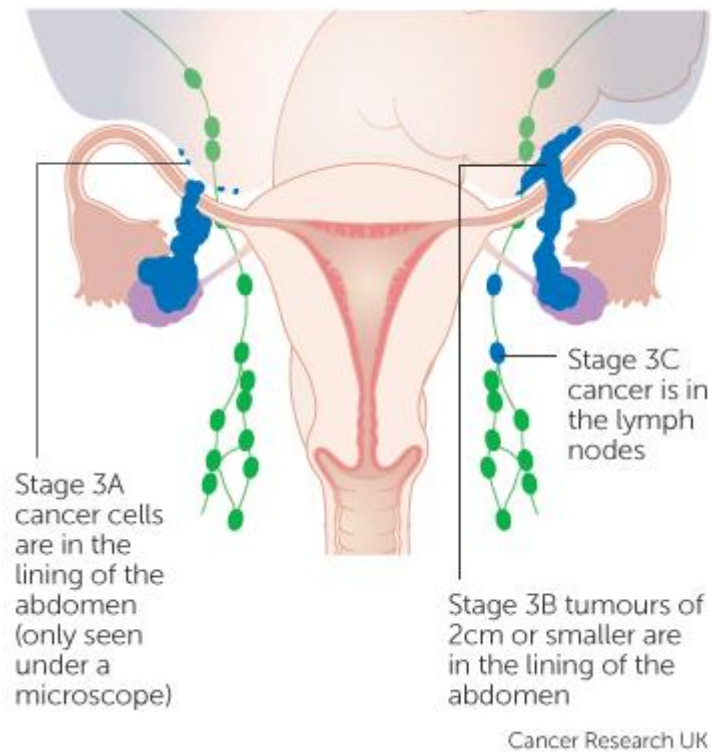
- 1,613 new cases diagnosed
- 1,069 deaths estimated



FIGO Stages



FIGO Stages



From Proteomics to Glycomics

- Matrix-assisted laser desorption ionization (MALDI)-mass spectrometry imaging (MSI)
- Formalin-fixed paraffin embedded (FFPE) tissue = high sample number and long term storage
- Introduction of **glycosylation** research



Glycosylation

There are two main types of glycosylation:

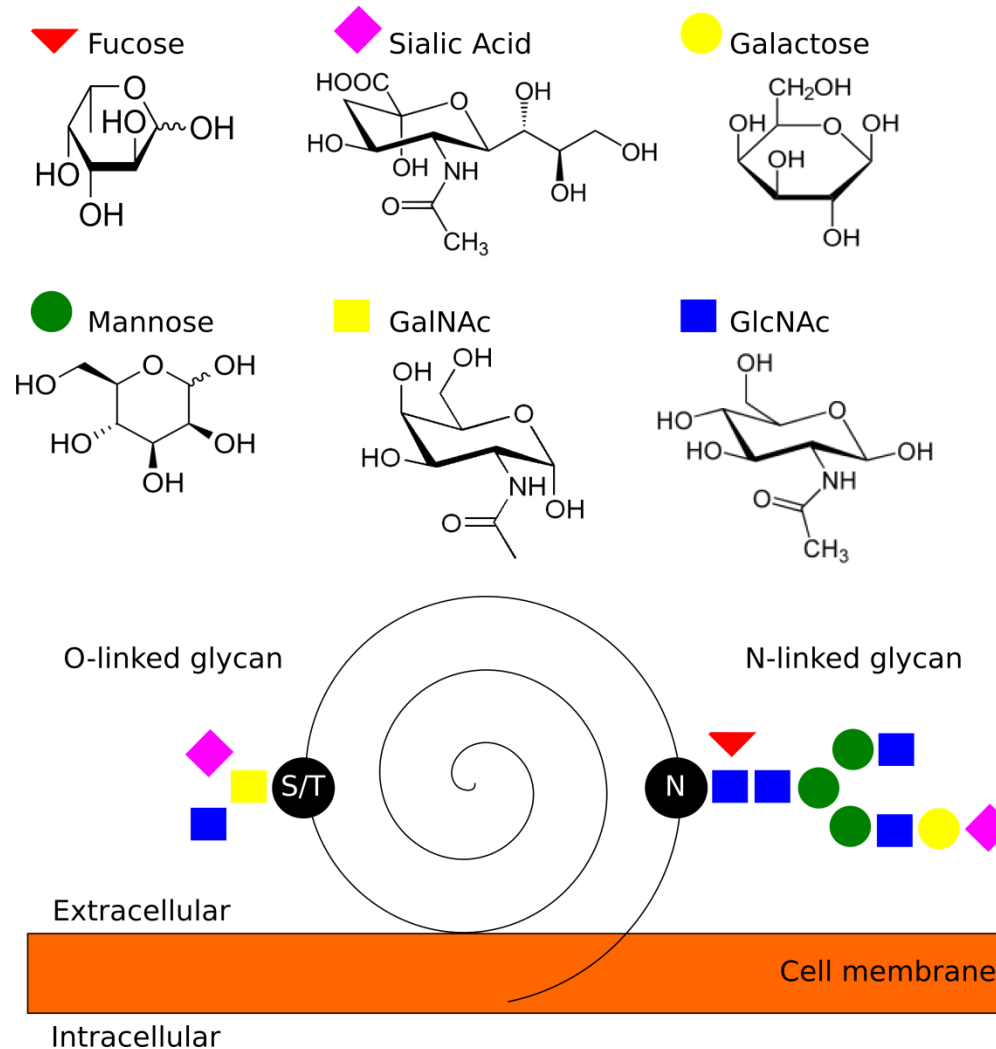
- *N*-linked glycosylation (attached to asparagine residues)
- *O*-linked glycosylation (attached to threonine or serine residues)

N-linked glycosylation is the most common with 90% of glycoproteins presenting *N*-glycans

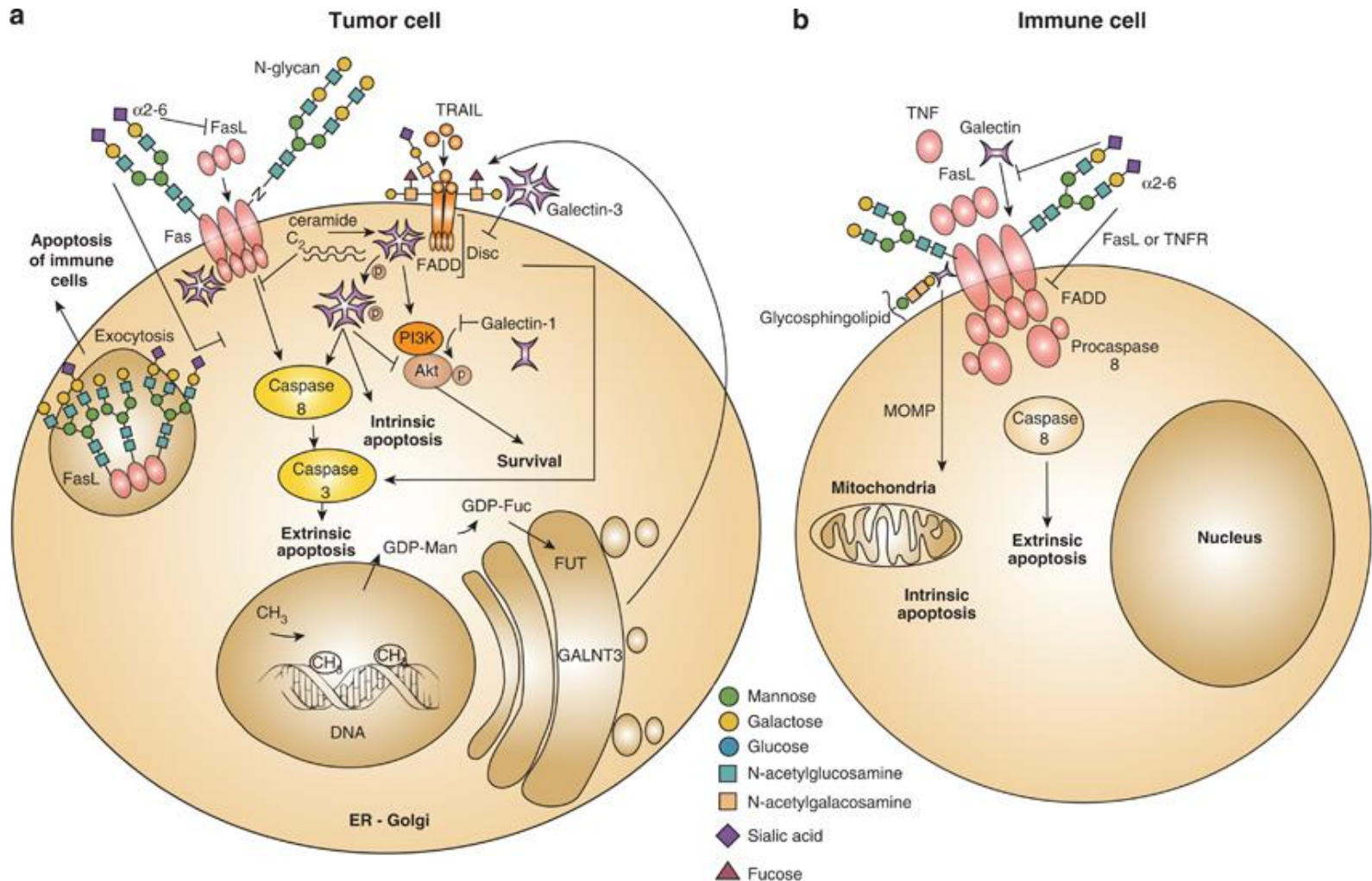
N-glycan structures have been observed to be altered in the tumour microenvironment, which contributes to metastasis



Protein Glycosylation

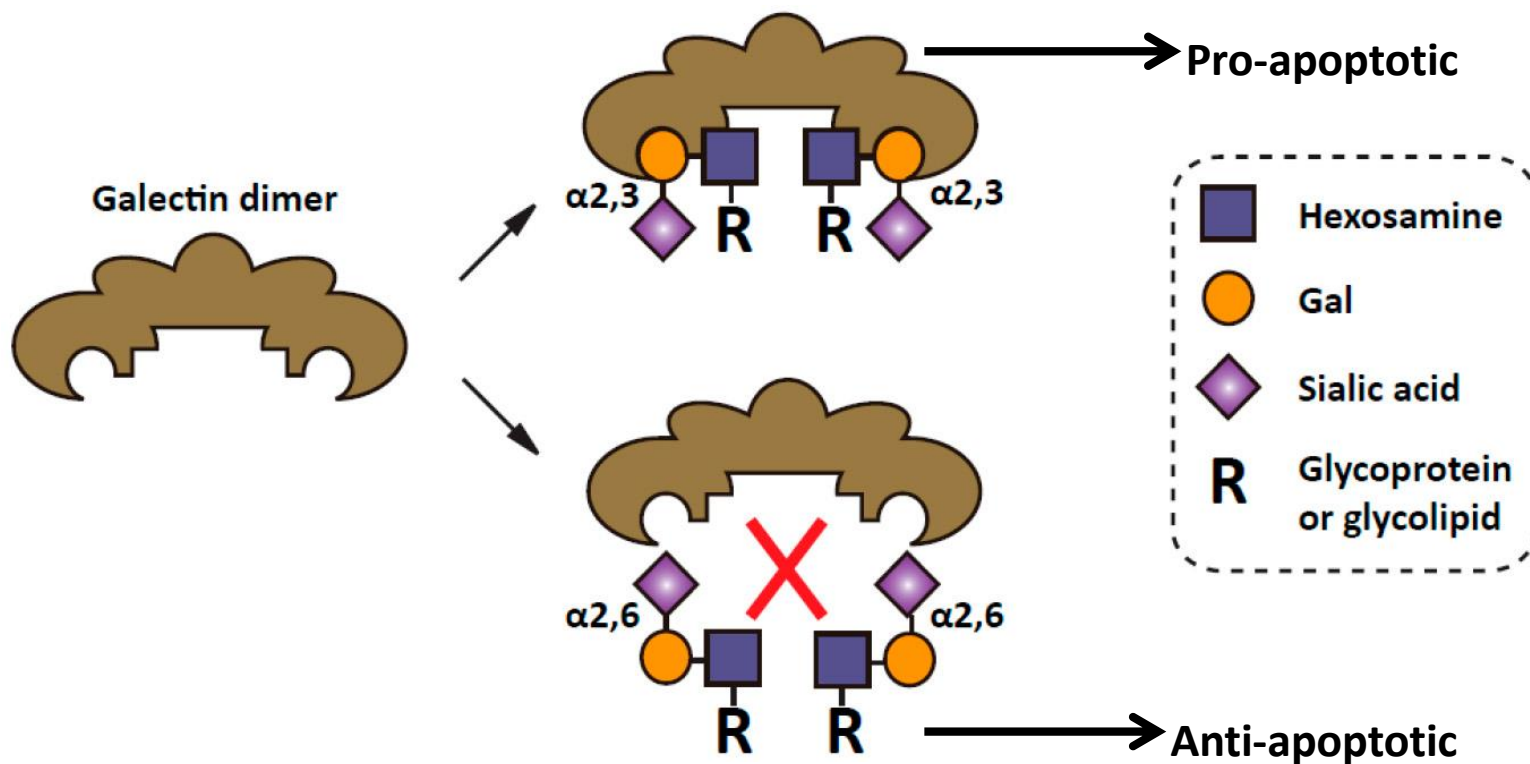


Glycosylation in apoptotic pathways



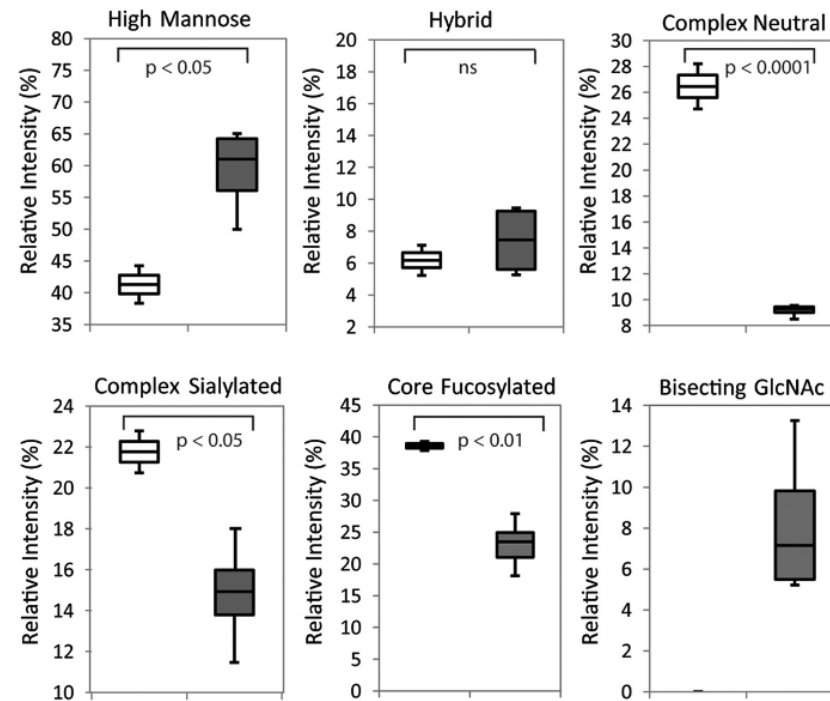
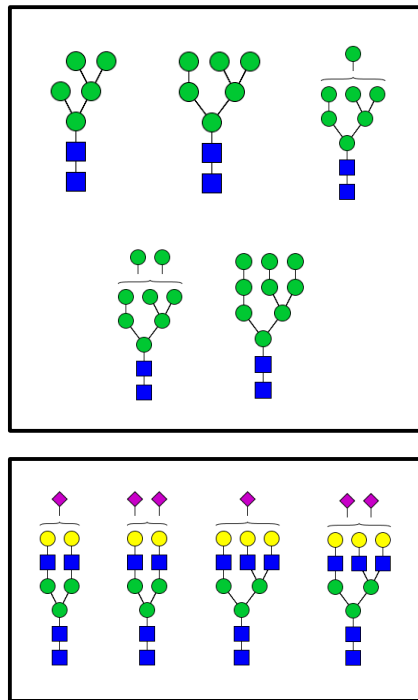
Cell Death and Differentiation (2013) **20**, 976–986; doi:10.1038/cdd.2013.50

α 2-6 Sialylation prevents apoptosis



Molecules **2015**, *20*, 7509–7527; doi:10.3390/molecules20057509

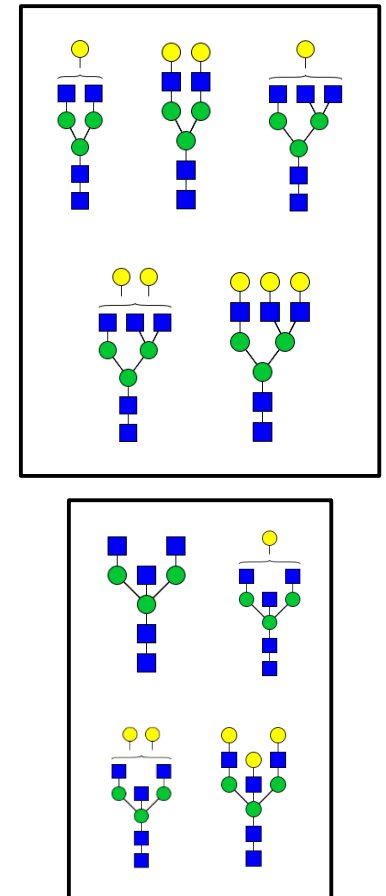
Ovarian Cell Lines: Healthy vs. Cancerous



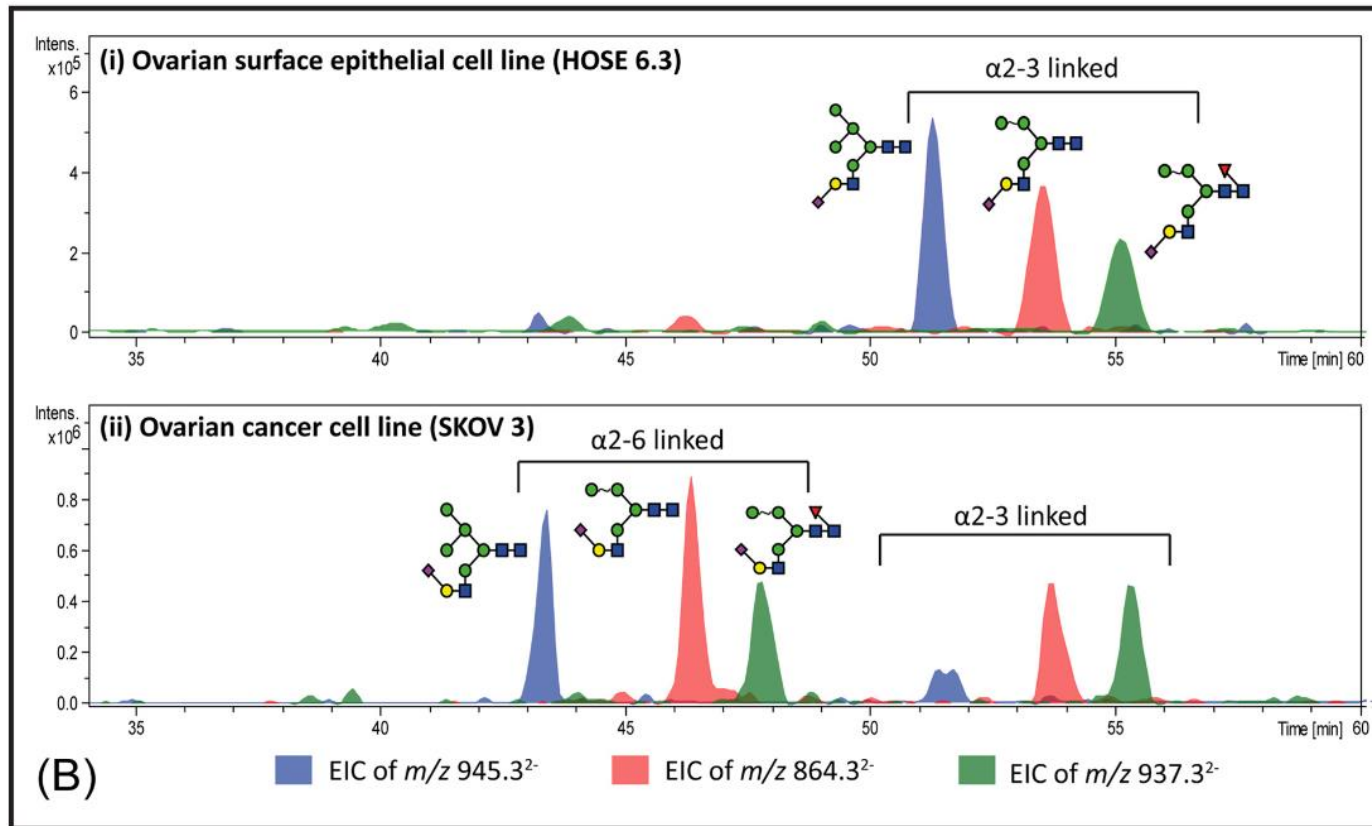
□ Non-cancerous ovarian surface epithelial cells (n=2)

■ Ovarian cancer cells (n=4)

ns: non-significant



Ovarian Cell Lines: Healthy vs. Cancerous

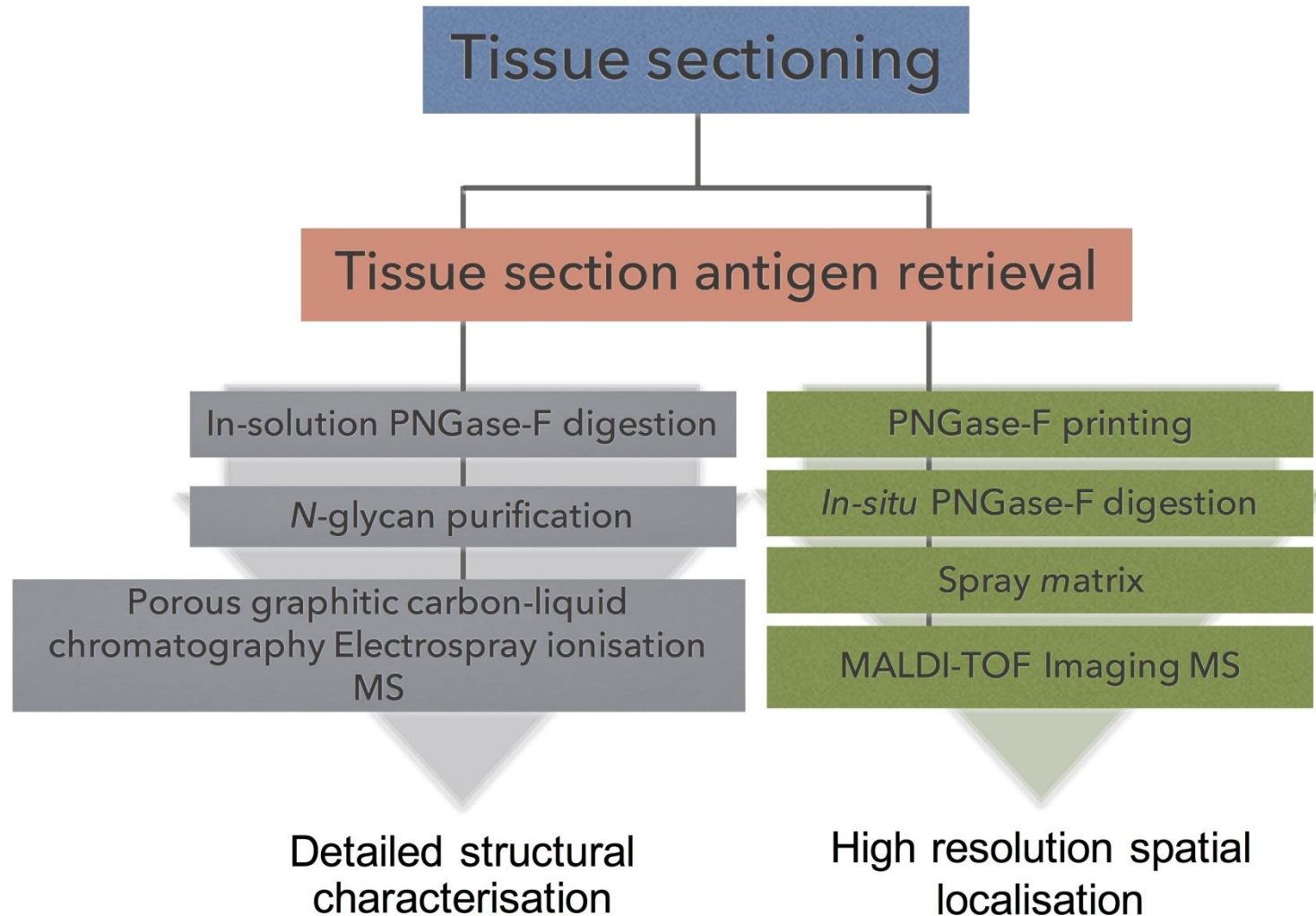


Questions

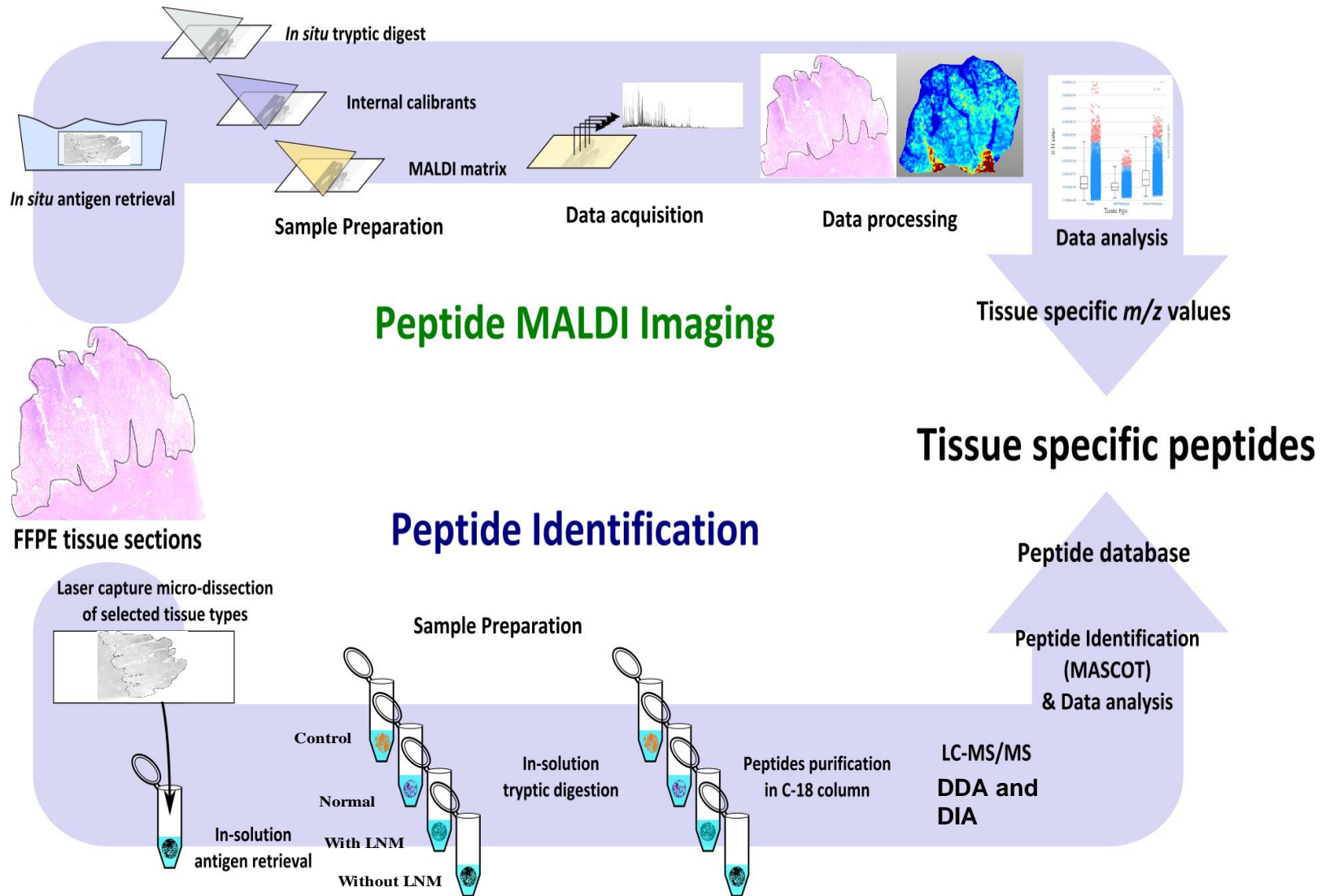
- Can the tumour, stroma and adipose regions of late-stage ovarian cancer tissue sections be differentiated based on the *N*-glycosylation pattern alone?

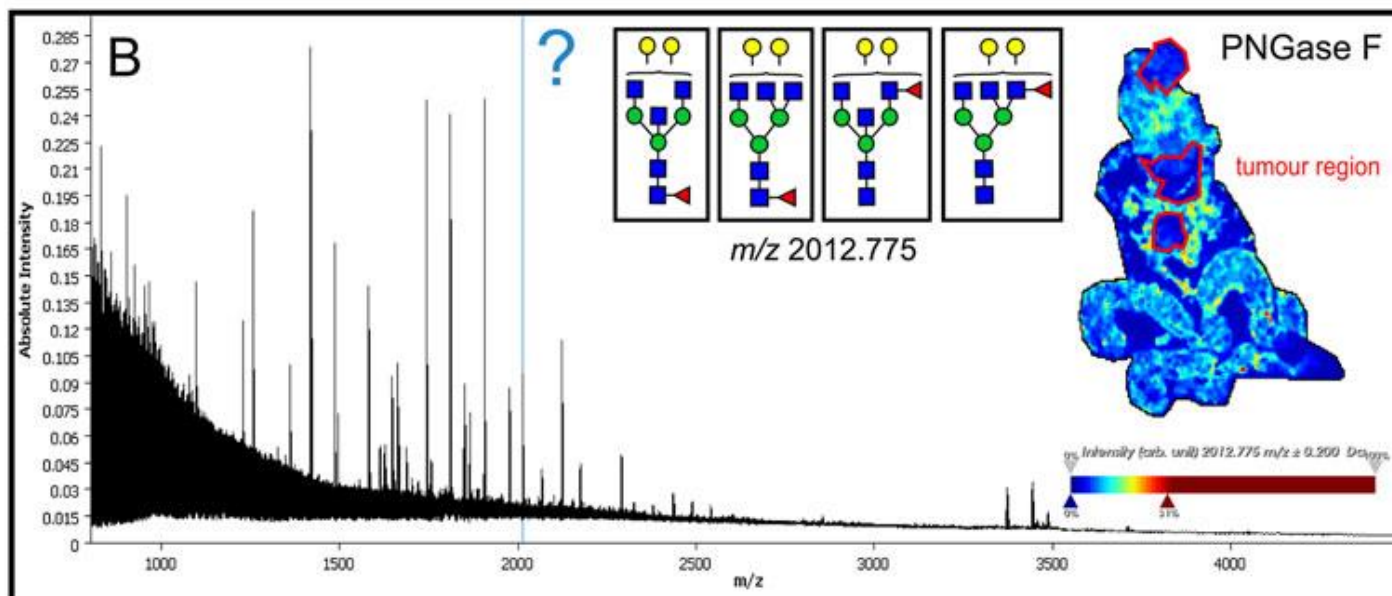
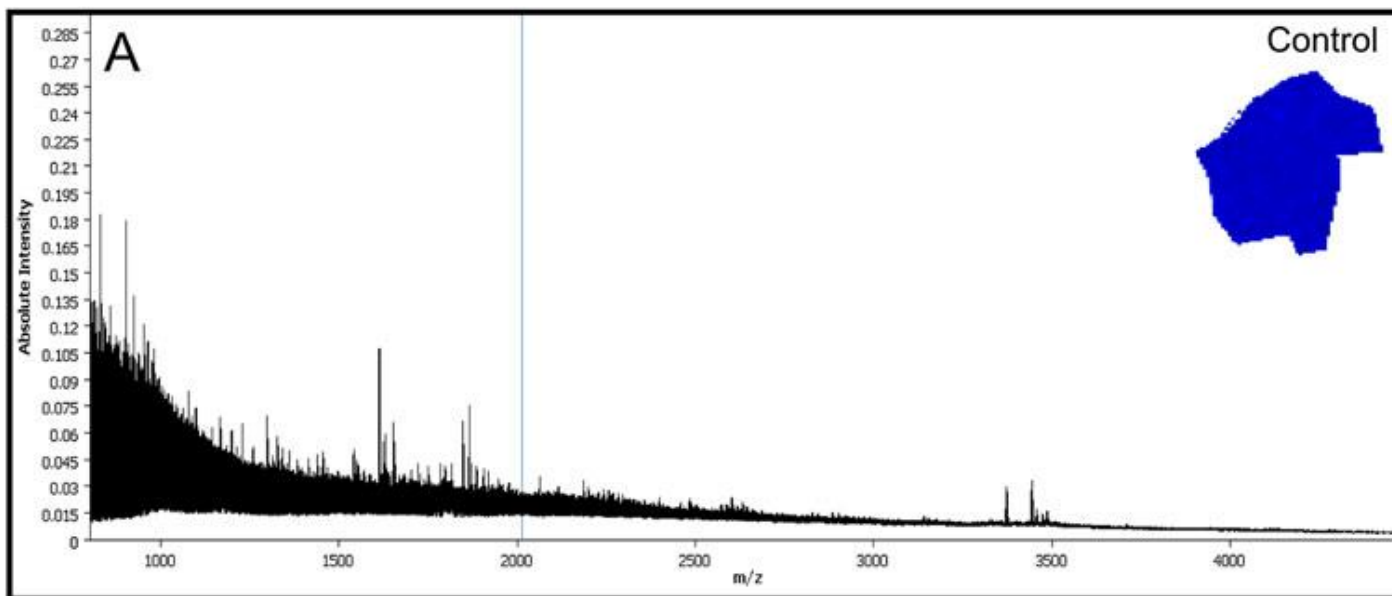


Workflow of *N*-glycan Imaging

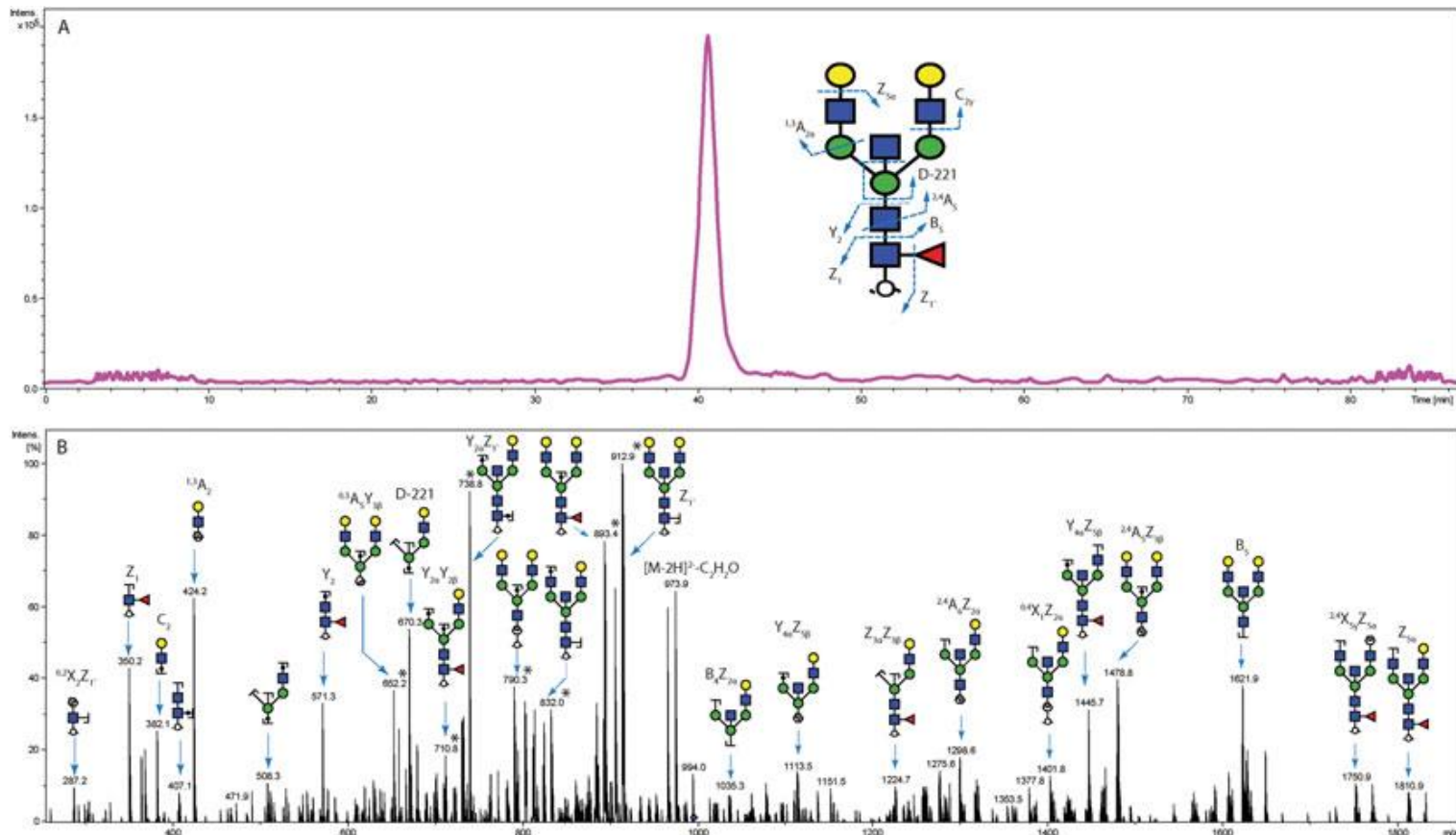


MALD Imaging of FFPE tissue sections



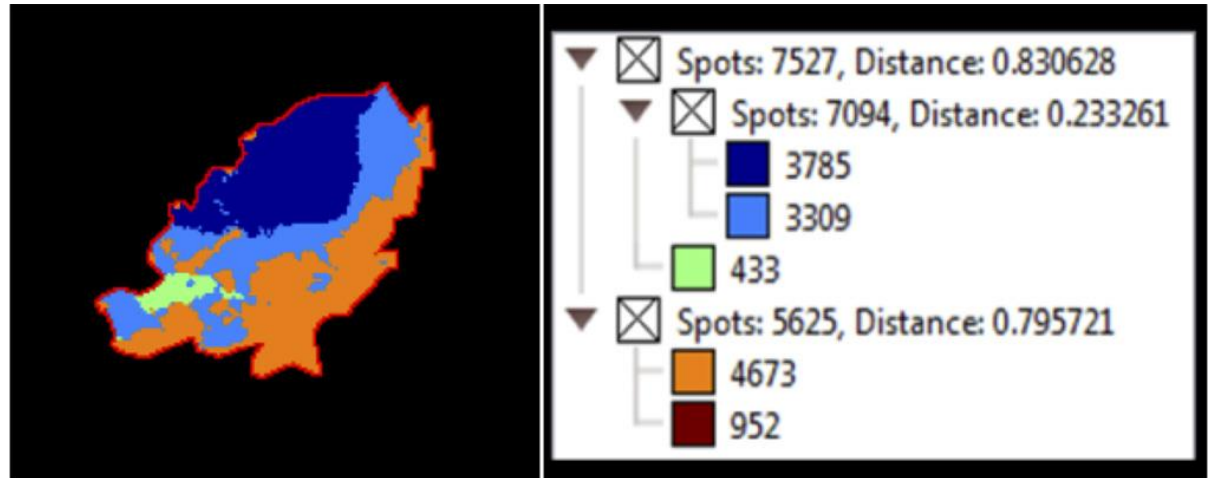
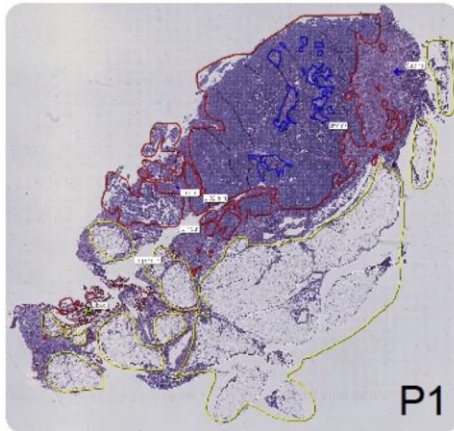


LC-MS/MS: Bisecting *N*-Glycan

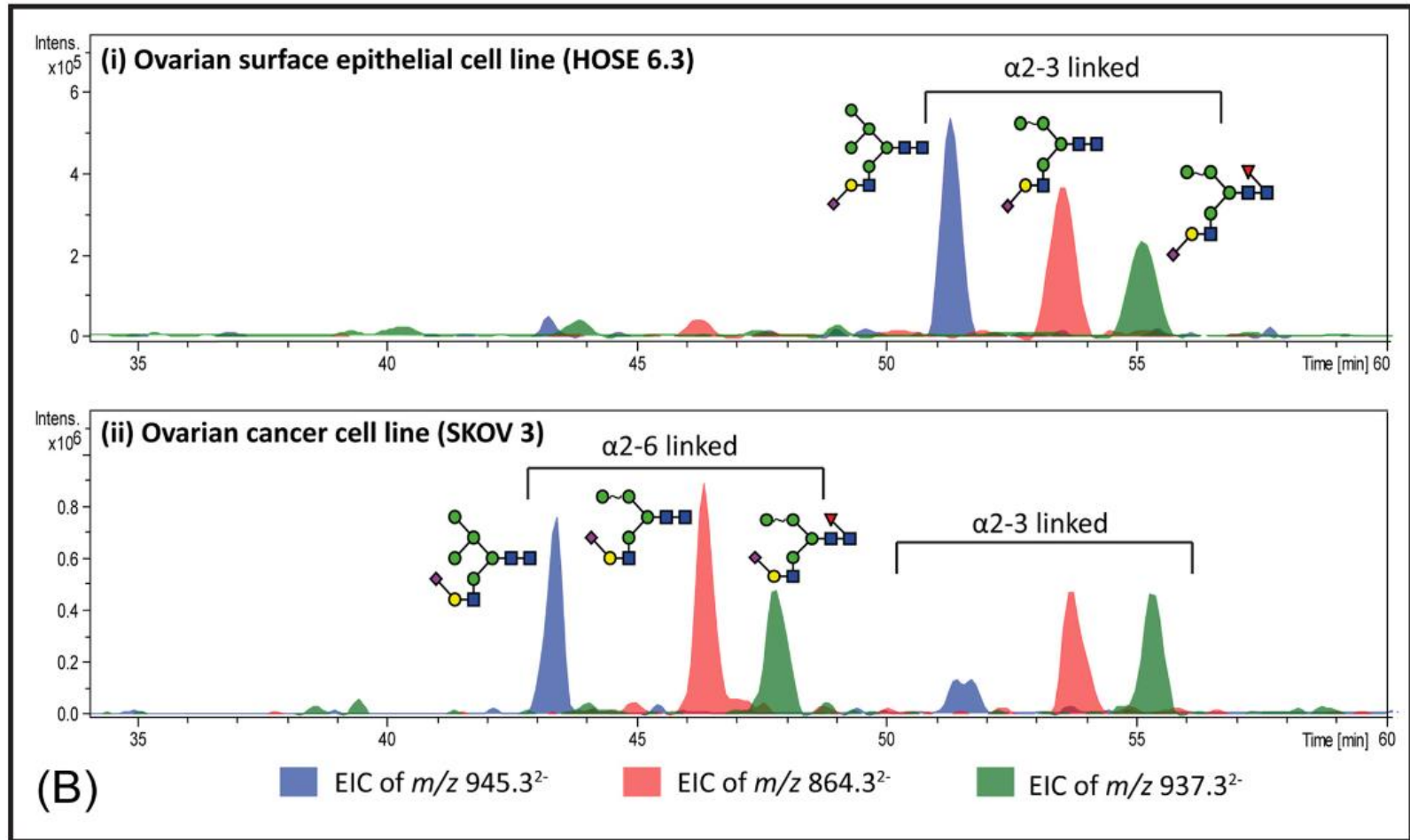


Another Stage IIIC Ovarian Cancer Patient: Segmentation Map

- Tumour
- Stroma
- Adipose

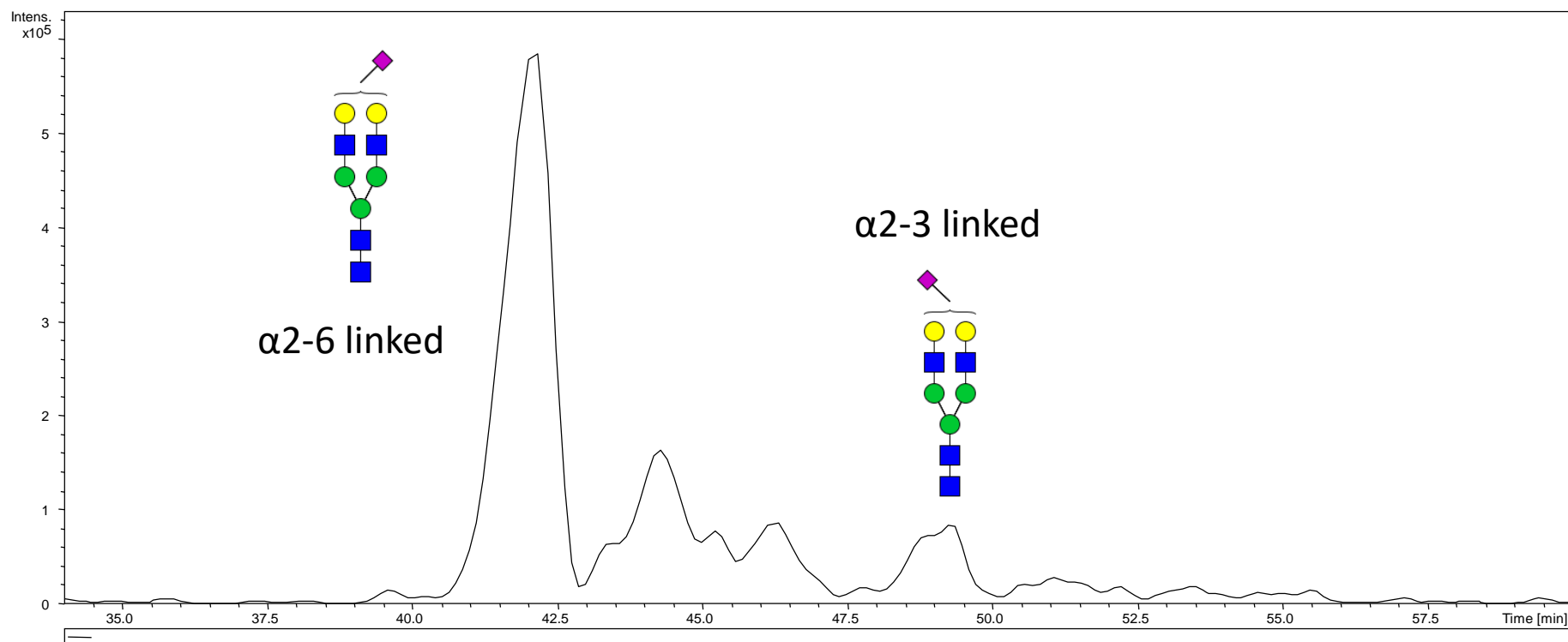


Sialylation in ovarian cell lines



[Mol Cell Proteomics](#). 2014 Sep;13(9):2213-32. doi: 10.1074/mcp.M113.037085.

Sialic acid linkages from tumor tissue

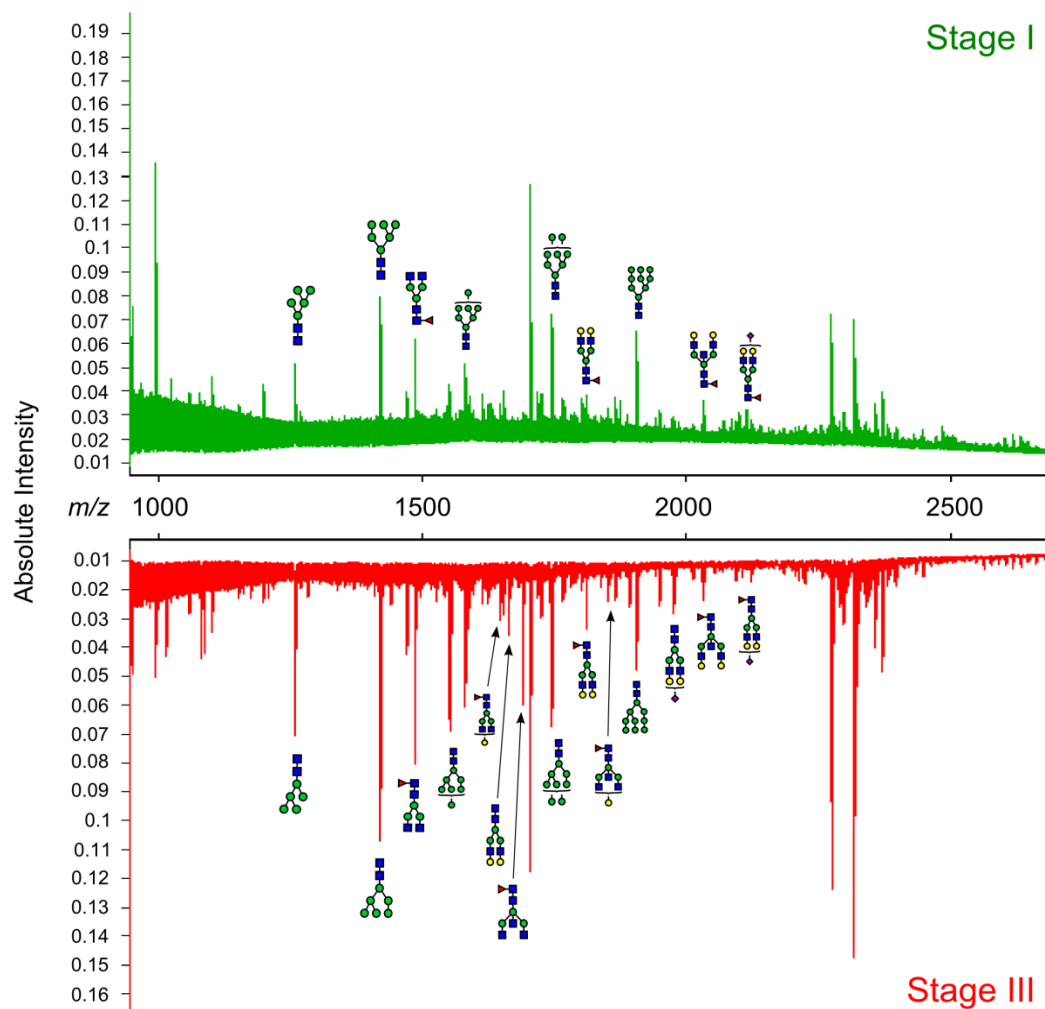


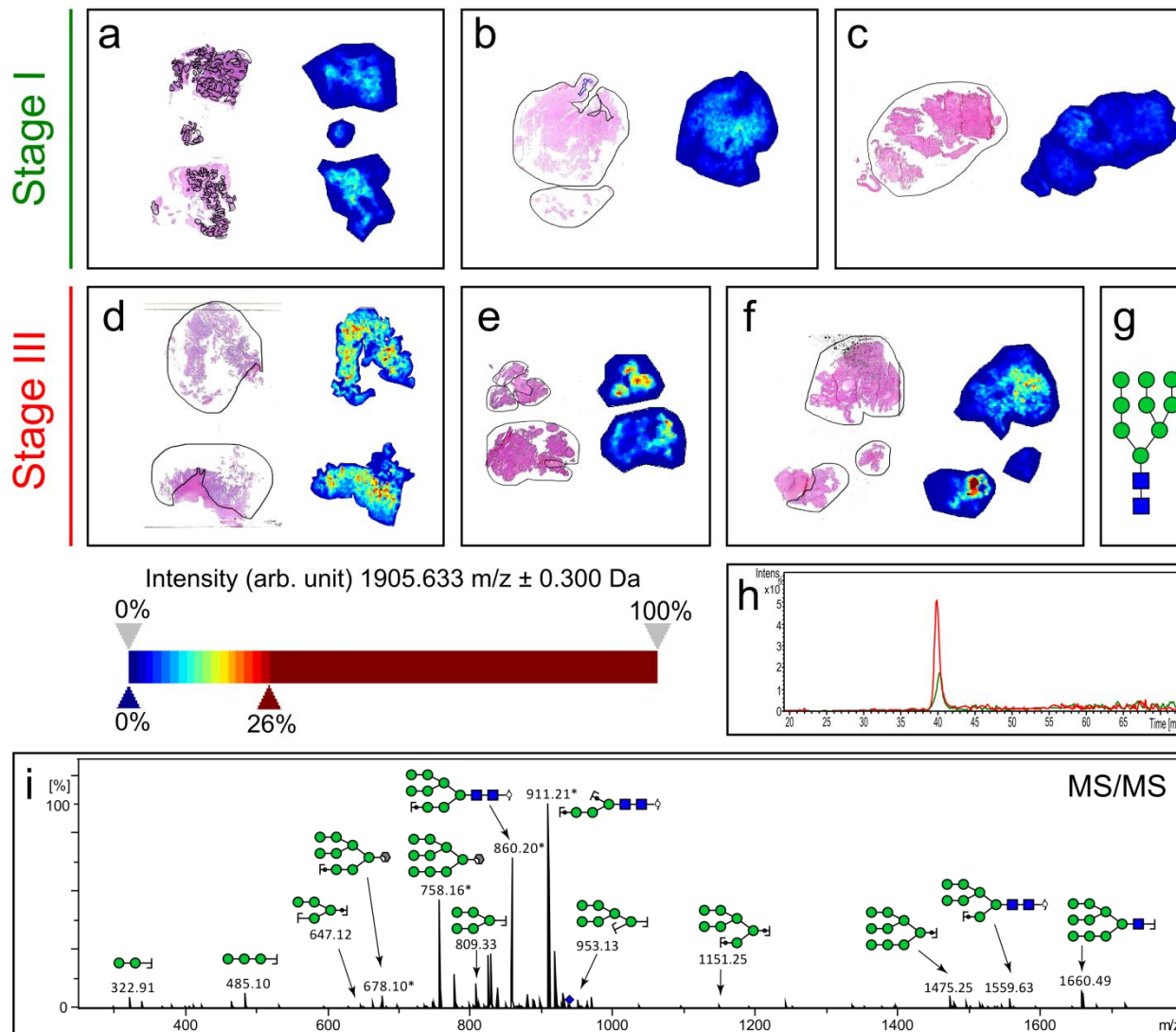
Questions

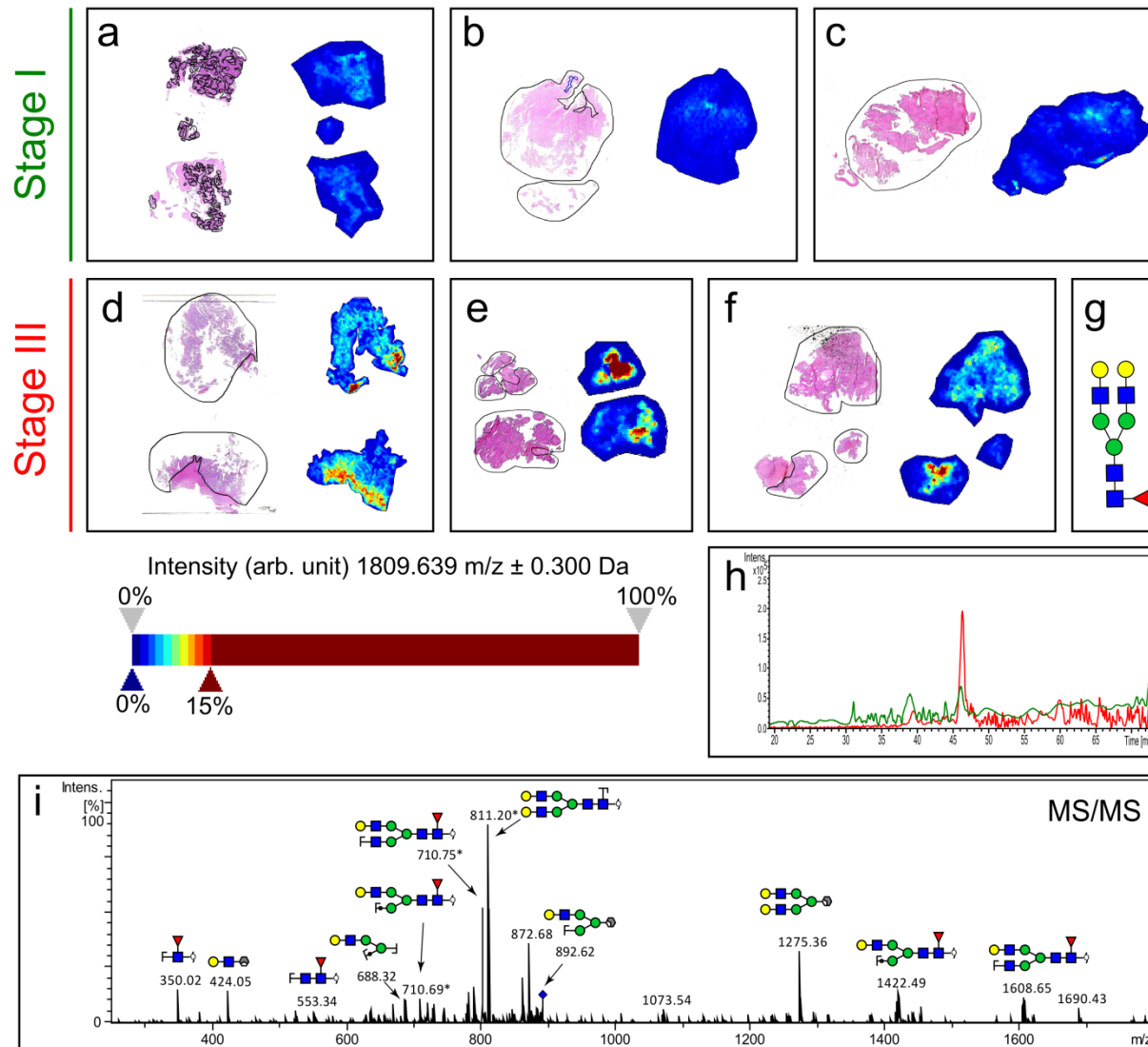
- Can early- and late-stage ovarian cancer tissue sections be differentiated based on the *N*-glycosylation pattern alone?

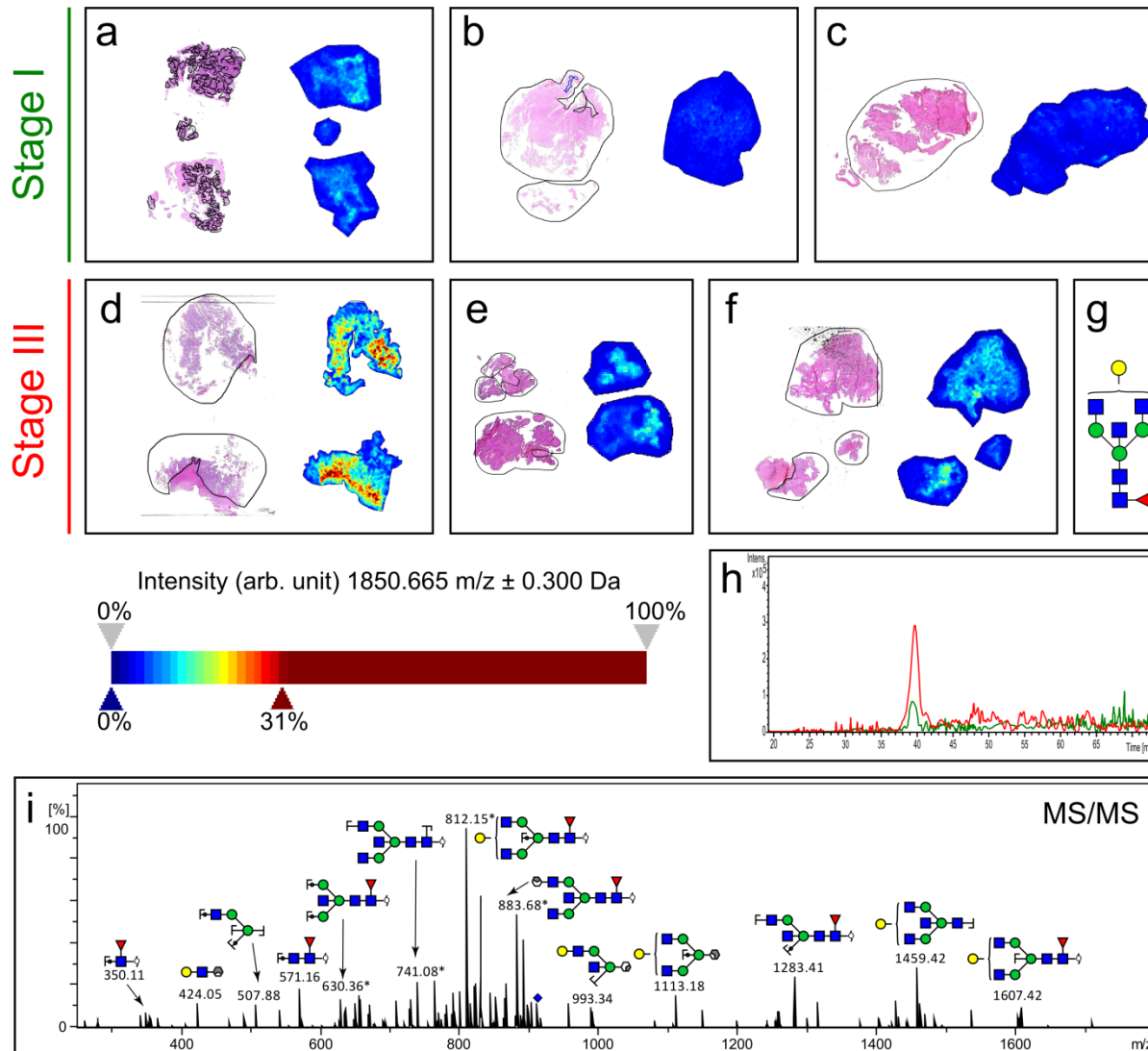


MALDI Sum Spectra: Stage I vs. Stage III









Summary

Increased *N*-glycans in late-stage tumour regions relative to early-stage tumour regions:

- High mannose
- Complex/fucosylated
- Bisecting

However, a larger cohort of patients (tissue microarray) is required



Overall Summary

Overall, our group has successfully:

- Established a *N*-glycan MALDI-MSI workflow with complimentary LC-MS/MS of consecutive sections
- Applied our *N*-glycan MALDI-MSI workflow to FFPE ovarian cancer to answer clinical questions
- Discovered *N*-glycan differences between early- and late-stages ovarian cancer patients that could lead to the potential discovery of a novel diagnostic marker



MALDI Imaging on *N*-glycans

Gustafsson OJ, **Briggs MT**, Condina MR, Winderbaum LJ, Pelzing M, McColl SR, Everest-Dass AV, Packer NH, **Hoffmann P**. MALDI imaging mass spectrometry of N-linked glycans released from formalin-fixed murine kidney. *Anal & Bioanal Chem.*, **2015**, 407, 2127-2139

M.T. Briggs, J.S. Kuliwaba, D. Muratovic, A.V. Everest-Dass, N.H. Packer, D.M. Findlay, **Peter Hoffmann**. MALDI mass spectrometry imaging of N-glycans on tibial cartilage and subchondral bone proteins in knee osteoarthritis. *Proteomics*, **2016**, 16(11-12):1736-41.

A.V. Everest-Dass*, **M.T. Briggs***, K. Gurjeet, M.K. Oehler, **P. Hoffmann***, N.H. Packer*. N-glycan MALDI imaging mass spectrometry on formalin-fixed paraffin-embedded tissues enables the delineation of ovarian cancer tissues. *MCP*, **2016**, 15(9): 3003-3016.

M.T. Briggs, Y.Y. Ho, G. Kaur, M.K. Oehler, A.V. Everest-Dass, N.H. Packer, **P. Hoffmann**. 2N-glycan matrix-assisted laser desorption/ionization mass spectrometry imaging protocol for formalin-fixed paraffin-embedded tissues. *Rapid Communication in Mass Spectrometry*. **2017** May 30;31(10):825-841.



Acknowledgements

Proteomics and MS group

- **Dr. Georgia Arentz**
- Dr. Mark Condina
- Dr. Manuela Klingler-Hoffmann
- Dr. Yin Ying Ho
- Dr. Noor Lackman
- Chris Cursaro
- **Parul Mittal**
- Chao Zhang
- **Matthew Briggs**
- Lyron Winderbaum
- Michelle Turvey
- Mitch Acland
- Brooke Dilmetz

Royal Adelaide Hospital

- **Prof. Martin K. Oehler**
- Dr. Carmela Riccardelli

Macquarie Univervisty

- **Prof. Nicole Packer**
- **Dr. Arun Dass**

University Sains, Malaysia

- **Prof Gurjeet Kaur**

